

Wetland shear strength with emphasis on the impact of nutrients, sediments, and sea level rise[☆]

Navid H. Jafari^a, Brian D. Harris^{a,*}, Jack A. Cadigan^a, John W. Day^b, Charles E. Sasser^b, G. Paul Kemp^b, Cathleen Wigand^c, Angelina Freeman^d, Leigh Anne Sharp^d, James Pahl^d, Gary P. Shaffer^e, Guerry O. Holm Jr.^f, Robert R. Lane^g

^a Department of Civil and Environmental Engineering, Louisiana State University, USA

^b Department of Oceanography & Coastal Sciences, Louisiana State University, USA

^c U.S. Environmental Protection Agency, USA

^d Louisiana Coastal Protection and Restoration Authority, USA

^e Department of Biological Sciences, Southeastern Louisiana University, USA

^f Jacobs, Senior Technologist, USA

^g Comite Resources, Inc., USA

ARTICLE INFO

Keywords:

Effective stress
Pore-water pressure
Total stress
Density
Vane shear
Cone penetrometer
Torvane
Shear strength
Vegetation
Roots

ABSTRACT

This paper presents a comprehensive review of shear strength measurements in wetland soils, which can be used to make inferences of the influence of nutrients and sediments on wetland health. Ecosystem restoration is increasing across the Gulf of Mexico and in other coastal systems, with management questions related to soil strength among the most critical to address for the sustainability of restoration programs. An overview of geotechnical engineering principles is provided as a starting point to understand basic soil mechanics concepts of stress, effective stress, pore-water pressure, unit weight, and shear strength. The review of wetland shear strength measurements focuses on the hand-held vane shear, torvane, cone penetrometer, and wetland soil strength tester. This synthesis shows that vane shear measurements can identify the shear strength trend in horizontal and vertical spaces and may be an indicator of wetland soil strength. However, the significant uncertainty of the vane shear measurements may preclude making conclusions about shear strength values without further testing and calibration of the devices. The torvane results show considerable scatter such that it is not recommended for quantitative shear strength measurements. The cone penetrometer represents a technique that is independent of operators and provides a high density of measurements with depth. It signifies the state-of-practice of wetland shear strength testing and is a reasonable tool to measure spatial and temporal variations in soil strength and other geotechnical properties (e.g., pore-water pressure, soil moisture, resistivity, and temperature) in wetlands. The wetland soil strength tester provides insight into the wetland soil resistance in the first 15 cm, which is the zone where most belowground biomass is present. Recommended future research includes evaluating the uncertainty in all *in-situ* soil strength testing methods, developing relationships between different field instruments, and establishing consistent statistical methods and field-testing procedures to make inferences and assessments.

1. Introduction

The importance of geotechnical properties on the dynamics of coastal wetland sustainability is underscored by the many

investigations in the Mississippi Delta and elsewhere that explain the mechanisms contributing to marsh edge erosion, shallow subsidence, and wetland collapse (Knutson et al., 1988; Pestrong et al., 1972; Redfield et al., 1972; Day et al., 1998, 2007, 2012, 2016; Syvitski et al.,

[☆] A review paper submitted for publication in a special issue on freshwater introductions in *Estuarine, Coastal and Shelf Science*.

* Corresponding author.

E-mail addresses: njafari@lsu.edu (N.H. Jafari), bharr96@lsu.edu (B.D. Harris), jcadig1@lsu.edu (J.A. Cadigan), johnday@lsu.edu (J.W. Day), csasser@lsu.edu (C.E. Sasser), gpkemp@lsu.edu (G.P. Kemp), Wigand.Cathleen@epa.gov (C. Wigand), angelina.freeman@la.gov (A. Freeman), leighanne.sharp@la.gov (L.A. Sharp), james.pahl@la.gov (J. Pahl), shafe@selu.edu (G.P. Shaffer), guerry.holm@jacobs.com (G.O. Holm), rlane@comiteres.com (R.R. Lane).

<https://doi.org/10.1016/j.ecss.2019.106394>

Received 17 April 2019; Received in revised form 30 August 2019; Accepted 17 September 2019

Available online 25 September 2019

0272-7714/ © 2019 Elsevier Ltd. All rights reserved.

2009; Couvillion et al., 2017; Bondoni et al., 2014, 2016; Cola et al., 2008; Coops et al., 1996; Howes et al., 2010; Mariotti and Fagherazzi, 2010; Fagherazzi et al., 2012). Considerable discussion over the past decade has focused on the effects of nutrient and sediment loading and other factors on coastal wetlands with regard to belowground biomass productivity, soil strength, and soil organic matter decomposition (Darby and Turner, 2008a,b,c; Fox et al., 2012; Anisfeld and Hill, 2012; Day et al., 2009, 2011, 2013, 2018; Deegan et al., 2012; Graham and Mendelsohn, 2014; Morris et al., 2013a; Nyman, 2014; Quirk et al., 2019; Swarzenski et al., 2008; Turner, 2011; VanZomeren et al., 2011; Shaffer et al., 2015). In particular, nutrient loading to coastal wetlands may cause decreased belowground productivity and soil strength and increased soil organic matter decomposition, which decreases wetland resilience to disturbance (Darby and Turner, 2008a,b,c; Deegan et al., 2012). The motivation and outcome of this review is predicated on the many ongoing efforts to understand wetland soil strength, how it varies across space and time, and how soil structure will respond to various restoration techniques.

With increasing threats to coastal systems and communities, ecosystem restoration and protection efforts are being undertaken in the Gulf of Mexico region and in other coastal systems to a scale that has not previously been realized. For example, Couvillion et al. (2017) estimated that more than 4800 square kilometers of coastal wetlands in Louisiana were converted to open water between 1932 and 2016, due to a wide variety of natural and anthropogenic causes. Predictive modeling for the LA State 2017 *Comprehensive Master Plan for a Sustainable Coast* (CPRA, 2017) suggests that an additional 10,000 + square kilometers could be lost, depending on presumptions of future riverine and marine processes, storm events, climate change, nutrient management, and population growth. A large-scale restoration and protection effort is underway, with Louisiana's 50 year, \$50 billion *Comprehensive Master Plan for a Sustainable Coast* (CPRA, 2017), including a portfolio of protection and restoration projects to reduce land loss and preserve coastal environments and communities. The restoration and protection of coastal systems is an emerging science, with questions around how to best quantify soil characteristics and how to increase understanding of the impact of nutrients and sediments on wetland soil strength being some of the most critical to address. Management questions related to soil strength vary by type of landscape (e.g., marsh or barrier island) and by types of restoration and protection projects. For river diversion projects that connect the river to the wetlands, improved understanding of soil strength and erodibility of sediments and soils in the receiving basins for the diversions is important for predicting marsh and water bottom erosion. The response of the bay bottom to the loading of newly deposited sediments is also of interest. In wetland areas, the strength of the marsh soils and the predicted response to the input of sediment and nutrients is important for effective management. Quantifying shear strength of soils is also essential for predicting the stability of shoreline stabilization and protection projects such as levees, floodwalls, and surge barriers. Quantitative measurements of soil strength are important for developing baseline conditions and tracking changes over time, as well as being valuable for the parameterization of Coastal Master Plan and other numerical models being used to inform coastal restoration and protection decision making.

Coastal areas in Louisiana are challenging to restore and protect due in part to the large quantity of soft alluvial soils in the landscape. Due to its deltaic origins, the landscape has alternating layers of silts, clays, and organics that are highly variable (Blum and Roberts, 2012). In addition, these wetland soils are highly complex due to their physical and hydraulic heterogeneity, fine layering, and unique structural properties (root mat development), presence of shells, and relatively low soil strengths. Tree and shrub roots are known to affect soil strength, e.g., mechanical reinforcement derived from large and fine roots acting as tensile reinforcement (Gray and Sotir, 1996). These root systems also affect soil hydrology by reducing water content through

evapotranspiration and increasing soil permeability (Collison et al., 1995; Gray and Sotir, 1996; Kim et al., 2013; Coops et al., 1996; Durocher, 1990; Meijer, 2015; Micheli and Kirchner, 2002; Pollen, 2007; Thorne, 1990; Van Eerd, 1985). In comparison, factors that alter wetland soils include vegetation species and root biomass (Turner, 2011), surface drainage and evapotranspiration (Day et al., 2011), and stratigraphy (Howes et al., 2010; Wigand et al., 2018). For example, Howes et al. (2010) suggested that a lens of inorganic material deposited by a deliberate levee breach during the 1927 flood was a contributor to wetland loss during Hurricane Katrina because this inorganic layer inhibited growth of abundant roots and rhizomes (see also Kearney and Rogers, 2010; Day et al., 2016). Snedden et al. (2015) reported that prolonged flooding, especially during the growing season, led to lower belowground biomass production that further weakened wetland soils in the Caernarvon outfall area. These wetland soils are highly sensitive and particularly difficult to sample in an undisturbed manner for laboratory experiments. Thus, *in-situ* or field test methods must be used to characterize the stratigraphy and mechanical behavior of wetland soils.

Standard geotechnical instruments used in practice were developed for site investigations of civil infrastructure projects and now are used to measure the shear strength of wetlands, including the hand-held vane device (Howes et al., 2010; Turner, 2011; Chen et al., 2013), torvane (Wilson et al., 2012; McGinnis, 1997), and cone penetrometer (Are et al., 2002; Day et al., 2011; Jafari et al. 2019). Other instruments developed from the outgrowth of research have aimed at understanding vegetation-soil properties. For example, Meijer et al. (2017a,b) proposed four different geometric shapes (blade, pull-up, pin vane, and corkscrew) based on geotechnical principles to quantify reinforced root resistance of forest roots within a depth of 30 cm. Sasser et al. (2018) developed the Wetland Soil Strength Tester (WSST), which measures the combined torque resistance when inserting four 15 cm pins. In another application, regional and federal agencies such as the United States Environmental Protection Agency (USEPA) are developing rapid assessment protocols to ascertain wetland condition (Mack, 2001; Fennessy et al., 2007; Wardrop et al., 2007; Collins et al., 2008; Nestlerode et al., 2009). These rapid assessments are based on the condition of the universal features that identify wetlands, e.g., hydrology, hydric soils, and wetland biotic communities (Fennessy et al., 2007). It was found that the soil assessment components are the least developed because of the vast extent of salt marshes and limited available field time. As a result, bearing capacity measurements (penetration depth and loading response) were used in the field to quantify physical characteristics of the marshes (Bertness and Miller, 1984; Bertness, 1991). These data were measured using a modified soil penetrometer constructed of a PVC pipe and slide hammer, similar to that used by Herrick and Jones (2002). Twohig and Stolt (2011) also developed a bearing capacity penetrometer (made from PVC pipe with a conical end) to measure and compare soil properties between two tidally restricted and two (paired) unrestricted salt marshes.

Two instruments historically employed in coastal Louisiana wetlands to gauge shear strength profiles are the cone penetrometer and rotating vane apparatus (i.e., hand-held vane and torvane). A direct comparison of these instruments is difficult because they measure the response of different physical soil behaviors, such as measuring soil strength by displacing soil at different depths, integrating over different areas (blade height and width) or in different directions (i.e., horizontal vs. vertical), and cutting roots during testing or penetration. In addition, soil strength in coastal marsh environments is expected to be typically more variable than other environments due to the variability of microbial and macroscopic organics, porewater chemistry, and widely varying grain-size distributions. This lack of a uniform assessment methodology creates uncertainty when comparing different investigations on marsh soils and adds complexity when attempting to draw broad conclusions.

This paper provides a comprehensive review on factors impacting

and the techniques used to measure wetland soil strength. We start with an overview of geotechnical engineering principles and terminology, such as effective stress and shear strength, to understand how soil strength measurements were developed and the purpose of these measurements before discussing wetland soil strength measurements. The discussion highlights methods of presenting shear strength data, advantages and disadvantages of the instruments, and areas of future research in method development and testing to establish a standardized methodology for assessing wetland soil strength.

2. Concept of effective stress

A major indicator of wetland health is the soil condition; thus, it is key to understand soil mechanics and behavior which starts from the formulation of the effective stress principle (Terzaghi, 1936). The effective vertical stress (σ'_v) in a saturated soil is equal to the total vertical stress (σ_v) minus the pore-water pressure (u), and stress acting in the water of the soil in all directions with equal intensity (Terzaghi et al., 1996), as shown in Eq. (1).

$$\sigma'_v = \sigma_v - u \quad (1)$$

The units of each variable in Eq. (1) are kilopascals (kPa) or kilonewtons per square meter (kN/m²). A *newton* (N) is determined by multiplying mass (kg) with the gravitational constant g (9.81 m/s²) to obtain $N = kg \frac{m}{s^2}$. A force (N) imparted over an area (m²) corresponds to a pressure or stress, and is referred to as a *pascal* ($Pa = \frac{N}{m^2} = \frac{kg}{m \cdot s^2}$). The variables σ'_v , σ_v , and u in Eq. (1) are reported in kPa or 1000 Pa. For example, σ'_v is equal to 8.19 kPa when σ_v and u are 18 kPa and 9.81 kPa, respectively.

The total vertical stress (σ_v) at any point in a soil profile is determined by the saturated unit weight (γ_{sat} , kN/m³) and thickness z (m) of all material above that point, including free water above the soil surface. Saturated bulk density (ρ_{sat} , kg/m³) and γ_{sat} are related through the gravitational constant g , i.e., $\gamma_{sat} = \rho_{sat}g = \frac{kg}{m^3} \frac{m}{s^2} = \frac{N}{m^2}$. Typical values of ρ_{sat} for peat, clay, and sand are 1100 kg/m³, 1600 kg/m³, and 2200 kg/m³, respectively (Holtz et al., 2011). The corresponding γ_{sat} for these three soil types are 10.8 kN/m³, 15.7 kN/m³, and 21.6 kN/m³, respectively. These soil densities and unit weights are especially relevant in Louisiana, because the Mississippi River delta is a transitional depositional environment and salinity values impact the densities and unit weights of soils. The γ_{sat} for distilled water is typically taken as 9.81 kN/m³ and 10.093 kN/m³ for sea water (Noorany, 1984). Thus in the earlier example, if σ_v is equal to 18 kPa and u is 10.093 kPa, σ'_v becomes 7.907 kPa instead of 8.19 kPa.

To illustrate calculating σ'_v , σ_v , and u , Fig. 1 shows a wetland soil profile wherein a 0.5 m peat layer with decaying vegetation roots ($z = 0.5$ m) overlays a 1 m thick interdistributary deltaic clay. Interdistributary clays are fluvial marine sediments derived from river discharge, deposited in the low elevation environments which lie between present and past deltaic lobes, may be surrounded by marsh, and are connected to the sea directly or by tidal channels (USACE, 1958; Coleman and Gagliano, 1960). The groundwater surface or water table is at the ground surface (Fig. 1(a)), 0.3 m above ground surface (Fig. 1(b)), and 0.5 m below ground surface (Fig. 1(c)). In a hydrostatic condition such as Fig. 1(a)–(c), the rate of increase in pore-water pressure with depth is equal to the unit weight of water ($\gamma_w = \rho_w g$) multiplied by the depth z , where ρ_w is the density of water (1000 kg/m³). In other words, the pore-water pressure at any point in the soil is determined by the vertical distance of the water table above that point. For example, the pore-water pressure in Fig. 1(a) at a depth of 1.5 m is 14.7 kPa. The total stress at depth of 0.5 m and 1.5 m are 5.4 kPa and 21.1 kPa, respectively. The slope of σ_v changes at the interface of peat and clay layers because of the difference in γ_{sat} between the two layers. Moreover, the σ_v at 1.5 m is the summation of the total stress from the peat (5.4 kPa) and clay layer (15.7 kPa). Thus, σ'_v is computed last after

establishing σ_v and u with depth. Because the peat γ_{sat} is nearly equal to γ_w , the effective stress at depth of 0.5 m is approximately 0.5 kPa. Similar to σ_v , σ'_v increases more in the clay layer because of the higher γ_{sat} , approaching 6.4 kPa at a depth of 1.5 m. In Fig. 1(b), the groundwater level is increased to 0.3 m above the wetland surface to represent inundation from a combination of tides and cold fronts. The σ_v and u increase from 0 to 2.9 kPa at a depth of 0 m due to this ponded water. This is manifested in Fig. 1(b) by shifting the σ_v and u lines to the right. However, σ'_v remains the same between Cases I and II found in Fig. 1(a)–(b) because the increase in σ_v from the ponded water is offset by the increase in u by the same magnitude. One implication of Case II is that ponding more water on the wetland does not directly signify the soils will compress because the σ'_v does not concomitantly increase.

For Case III in Fig. 1(c), the water surface is lowered to the top of the clay layer. As a result, the pore-water in the peat layer is reduced to zero and the σ'_v increases to the same value as σ_v . As a result, σ'_v at a depth of 1.5 m is the highest in Case III compared to Cases I and II. In effect, lowering the groundwater surface increases σ'_v . An implication of Case III is that extended periods of groundwater lowering would be predicted increase the σ'_v and potentially cause soil consolidation, which was observed by Day et al. (2011) in Bayou Chitigue, LA. The magnitude of compression is related to magnitude of σ'_v increase so a slight change likely results in minimal consolidation, but extended periods of aeration can lead to shrinkage and desiccation of the vegetation layer, which increases the shear strength. The unit weight of the peat layer was assumed saturated for Case III, which is a safe assumption in Louisiana because of the frequent inundation. In other climates and regions, the evaporation of water from the soil will lead to a moist unit weight (γ_{moist}), which is slightly lower than γ_{sat} .

The conditions presented in Fig. 1 demonstrate how to estimate effective stress for a soil profile and fluctuating water levels. The effective stress can also change due to loading from structures (levees, roads, navigation locks) or natural hazards (e.g., ground shaking in earthquakes, storm surge and wave forcing during hurricanes) by increasing or decreasing the pore-water pressure (commonly referred to as excess pore-water pressure) from hydrostatic conditions. Understanding effective stress is important because measurable effects of wetland soil responses, such as compression, deformation, and strength, are due to changes in effective stress.

3. Concept of shear strength

The same factors involved within the design of bearing capacity of shallow and deep foundations, slope stability, and retaining walls that depend on soil strength are the same forces experienced by wetland soils. Shearing resistance in soils is the result of resistance at inter-particle contacts. Frictional resistance of soils results from sliding resistance and geometrical interference and interlocking (Terzaghi et al., 1996). Geometrical interference and interlocking is determined by the strength, size, shape, and arrangement of soil particles. In general, an increase in effective normal stress produces an increase of interparticle contact area and thus an increase in shearing resistance. Density is one important general indicator of shearing resistance, whereas porosity, void ratio, and water content reflect density of various types of soils (Terzaghi et al., 1996). The void ratio attainable under normal geologic and construction conditions is related mainly to the size, shape, surface characteristics, and strength of soil particles. The mineralogy of soil particles and the physiochemical environment influence shear resistance only indirectly through their control of these important particle characteristics. Increased density generally implies an increase in interparticle contact area and thus in shearing resistance. However, a unique relationship between density and shearing resistance is not to be expected for soils of different compositions because for any combination of density and effective stress, even in the absence of chemical bonding, different degrees of physical bonding are possible on account of differences in the nature of the soil particles (Terzaghi et al., 1996).

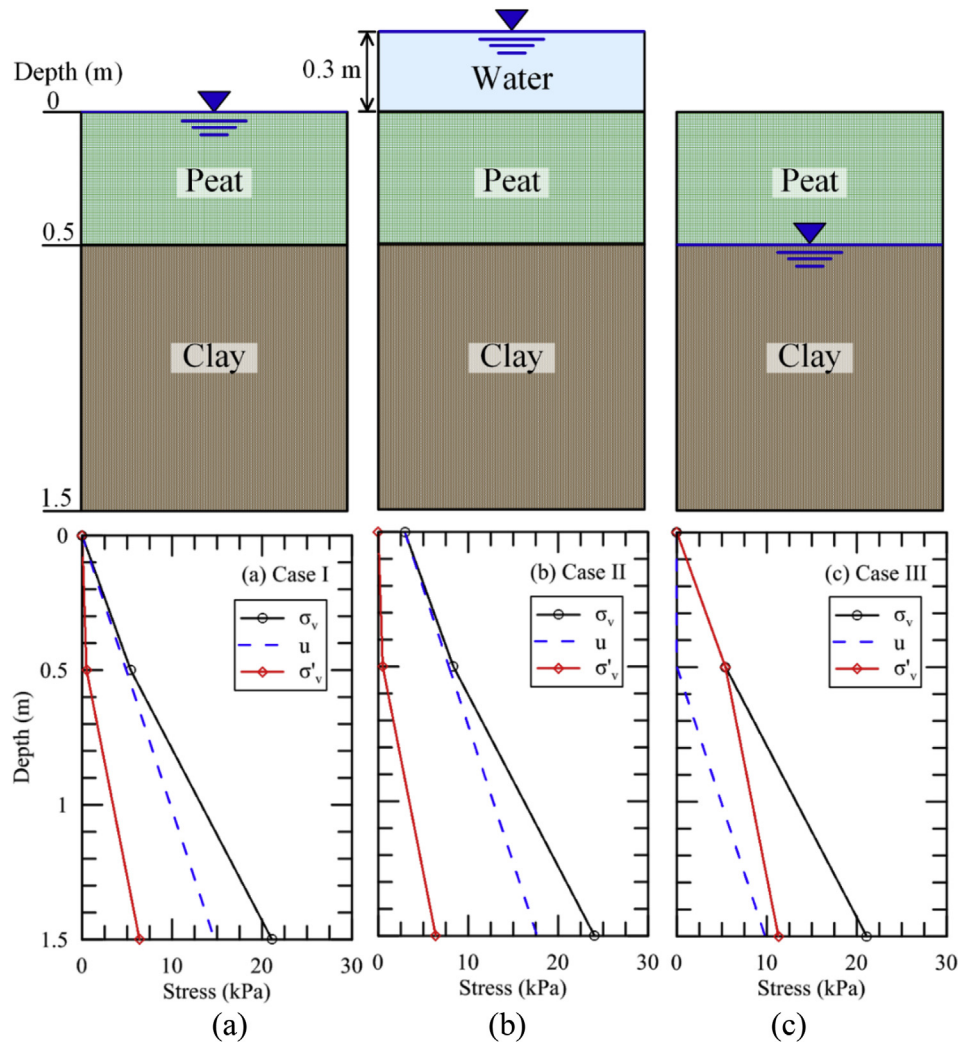


Fig. 1. Schematic of wetland soil profile with peat and clay layers with water levels at: (a) ground surface, (b) 0.3 m above ground surface, and (c) 0.5 m below ground surface. Legend: σ_v is the total vertical stress, u is the pore-water pressure, and σ'_v is the effective vertical stress.

With respect to wetland ecology, sediment is typically classified as mineral or organic and this will signify a range of bulk densities and correspond to a range of shear strength. Fig. 2(a) shows a power relationship between loss on ignition (i.e., organic matter content) and dry bulk density. For low organic contents less than 0.05 (i.e., mineral-dominated sediments), the dry bulk densities vary significantly from 0.9 g/cm³ to an upper limit of ~2 g/cm³. However, the dry bulk density decreases to ~0.1 g/cm³ as the organic content increases from 0.1 to 1. While Terzaghi et al. (1996) indicates that a unique relationship for density and shear strength does not exist, for wetland soils bulk density can be more of an indicator of shear strength because waterlogged organic or peat soils may not hold sufficient capacity to support itself, let alone permit someone to walk on it (DeLaune et al., 1994), when compared to mineral sediments. For example, Fig. 2(b) provides dry bulk densities for two sites in the LaBranche wetlands and two sites in the Bonnet Carré spillway. The LaBranche wetland is bordered by Lake Pontchartrain to the north while the rest of the area is bordered by flood control levees (Day et al., 2012). The major factors contributing to the deterioration of the LaBranche wetlands are isolation from riverine input by Mississippi River levees, hydrologic alterations, erosion, salt-water intrusion, hurricanes, semi-impoundment, nutria herbivory, and soil subsidence (Pierce et al., 1985; Day et al., 2012). In contrast, the Bonnet Carré spillway was opened only about once a decade, but accretion in the Bonnet Carré wetlands is almost an order of magnitude higher than in the LaBranche wetlands. Some areas of the Bonnet Carré

wetlands are nearly 2 m above sea level, consisting mostly of silts and sands. In Fig. 2(b), dry bulk density at the LaBranche two sites was between 0.20 and 0.30 g/cm³, which is typical of highly organic marsh soils receiving little mineral sediment input (DeLaune et al., 1978; DeLaune and Pezeshki, 1988). The Bonnet Carré soil profiles consisted of dry bulk density of over 1.0 g/cm³, which is typical of mineral soils with low organic matter content or a depositional environment with high sediment input (Day et al., 2012). The lower dry bulk density and evidence of deterioration at LaBranche suggests that the shear strength is also likely lower than the mineral-dominated Bonnet Carré wetlands, which can easily withstand vehicular traffic. Shear strength measurements in both wetlands can elucidate this hypothesis, and more broadly that dry bulk density (organic content) of only the sediment affects shear strength in wetland environments. With the current push for increased wetland restoration through sediment diversions, these relationships between dry bulk density and shear strength can serve as an indicator of future resistance levels a site has against erosive forces.

The Mohr-Coulomb strength envelope in Eq. (2) is the most widely used relationship for design of stability of natural and man-made slopes.

$$\tau = c' + \sigma'_n \tan(\phi') \quad (2)$$

where c' is the effective stress cohesion, σ'_n is the normal effective stress on the failure plane at failure, and ϕ' is the effective stress angle of internal friction. Selecting the appropriate shear strength parameters that reflects the *in-situ* conditions starts with understanding the

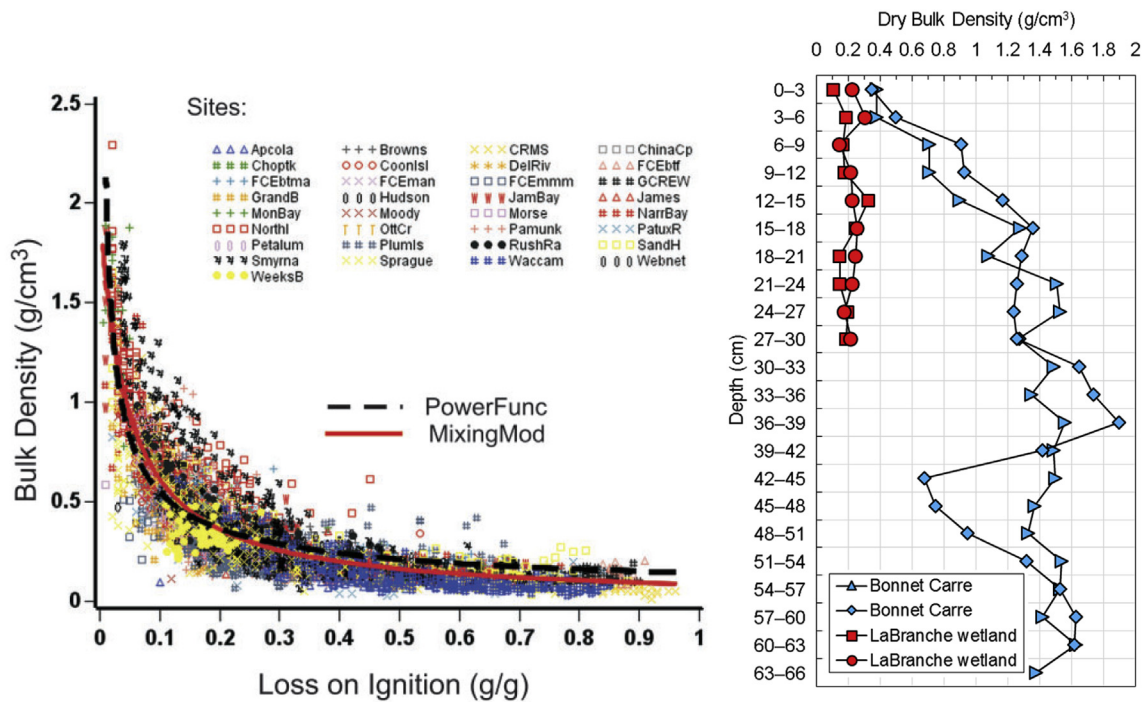


Fig. 2. (a) Relation between dry bulk density and loss on ignition (organic matter content) from 5075 sediment samples from 33 tidal marshes and mangroves distributed around the United States (Morris et al. 2002); (b) comparison of dry bulk densities from Bonnet Carré and LaBranche wetlands (data from Day et al., 2012).

concepts of drained and undrained conditions in relation to the mechanical behavior of soils. Both terms used in soil mechanics are related to hydraulic conductivity, in comparison with the length of time involved in loading or unloading the soil. If a storm surge of 3 m passes over a wetland, it is applying a normal stress on the wetland surface approximately equal to 29.5 kPa ($3\text{ m} \times 9.81\text{ kN/m}^3$) (assuming no stress is imparted from waves or surface currents). Once the storm surge recedes, the wetland is unloaded and the 29.5 kPa stress is removed. Thus, a storm surge may represent rapid loading and unloading (Howes et al., 2010). In comparison, levee construction over soft clays is also sufficiently rapid but the load remains over the service life of the infrastructure.

Drained conditions relate to water flowing into or out of a soil mass as rapidly as the soil is loaded or unloaded (consider water flowing around your feet while walking on the beach). A clay can also reach a drained condition over a long time period after loading because the excess pore-water pressures caused by loading dissipate (consider levees overlying soft clays many years after construction). In the field, drained conditions result when loads are applied to soil at a slow enough rate such that sufficient time is allotted for the dissipation of excess pore pressure back to a state of equilibrium (i.e. hydrostatic conditions) (Terzaghi et al., 1996). Sediment diversions can represent drained conditions for relic, highly organic soils in inactive delta lobes because the release of sediment-laden water slowly filtrates overland, raising water levels above the wetland surface slowly such that the soil can dissipate any excess pore-water pressure. In the laboratory, drained conditions are achieved by loading test specimens slowly so excess pore-water pressures do not develop as the soil is loaded. The drained strength is described by Eq. (2), but the effective cohesion term is assumed zero for normally consolidated saturated clays and organic soils (i.e., $\tau = \sigma'_n \tan(\phi')$), unless the saturated clay is overconsolidated, cemented, or contains roots that add tensile reinforcement (Terzaghi et al., 1996; Holtz et al., 2011).

In undrained conditions, no flow of water into or out of a soil mass occurs in response to load changes. Because water cannot escape, the applied load causes pore-water pressures to increase beyond hydrostatic

conditions (i.e., excess pore-water pressure). Undrained conditions may persist for days or weeks or months, depending on the duration of loading along with the soil hydraulic conductivity and compressibility and drainage conditions. In the field, undrained conditions result when loads are applied faster than the soil can drain. As pore-water pressures caused by loading dissipate over time, the soil mass can be said to transition from being under undrained conditions to drained conditions. This may occur during the construction of a marsh creation area, where dredged sediment is pumped into deteriorated marshes. In the laboratory, undrained conditions are achieved either by loading test specimens so rapidly that they cannot drain or by sealing them in impermeable membranes. The undrained shear strength (s_u) is also characterized by Eq. (2), but the friction angle is assumed zero so $\tau = c = s_u$. Undrained loading condition for wetlands is likely observed for marsh creation projects, waves impacting the marsh edge, and hurricane storm surge. Pore-water pressure measurements during these events may confirm undrained conditions are present. While hydraulic measurement are available from salt marshes in typical conditions (Nuttall and Hemond, 1988), measurements from hurricane passages over wetlands are focused on wave and surge attenuation (Mendez and Losada, 2004; Jadhav et al., 2013; Vuik et al., 2016) and the authors are not aware of any measured pore-water pressures in wetland soils.

The unit for shear strength is kPa (kN/m^2), which is the same as effective stress. Shear strengths are reported in g/cm^2 by various commercial brand torvanes and hand-held vanes. Eq. (3) shows the conversion procedure from kPa to g/cm^2 . In particular, the first line in Eq. (3) establishes the unit relations between kPa and Pa. The second line starts with $1000 \frac{\text{kg} \cdot \text{m}}{\text{m}^2 \cdot \text{s}^2}$ and involves dividing by the gravitational constant ($g = 9.81\text{ m/s}^2$) to convert from a force to a mass (kg). In line 3, the kg and m^2 are converted to g and cm^2 , respectively, to ultimately reach 10.2 g/cm^2 . For an example calculation, 400 g/cm^2 is equal to 40.7 kPa. It is recommended to report shear strength values in kPa to facilitate comparisons between studies.

$$\begin{aligned}
 1 \text{ kPa} &= 1 \frac{\text{kN}}{\text{m}^2} = 1000 \frac{\text{N}}{\text{m}^2} = 1000 \frac{\text{kg} \cdot \text{m}}{\text{m}^2 \cdot \text{s}^2} = 1000 \text{ Pa} \\
 1000 \frac{\text{kg} \cdot \text{m}}{\text{m}^2 \cdot \text{s}^2} &\times \frac{\text{s}^2}{9.81 \text{ m}} = 101.94 \frac{\text{kg}}{\text{m}^2} \\
 101.94 \frac{\text{kg}}{\text{m}^2} &\times \frac{1000 \text{ g}}{1 \text{ kg}} \times \frac{1 \text{ m}^2}{10,000 \text{ cm}^2} = 10.2 \frac{\text{g}}{\text{cm}^2}
 \end{aligned} \quad (3)$$

In geotechnical engineering applications, undrained and drained strengths are both evaluated because the designing engineer needs to estimate the performance for short- and long-term loading conditions. With respect to wetland ecology, shear strength is also used as a proxy for vegetation biomass or root density (Sasser et al., 2018) and erodibility of the marsh surface or underlying soils underlying the root zone by waves, storm surges, and overland flow (Pant, 2013; Allison et al., 2016). Changes in soil shear strength have been proposed to relate to changes in vegetation root mat due to environmental conditions such as hydroperiod, salinity, sediment deposition, and nutrients (Howes et al., 2010; Jafari et al., 2019). Thus, the objective is not determining drained or undrained strengths but rather identifying a reproducible, rapid, and accurate in-situ technique. Nevertheless, undrained conditions typically control design for soft clays and organic soils, so the standard geotechnical *in-situ* test methods (cone penetrometers and field vane) measure undrained strength s_u . This is also the case for prior studies of wetland soil strength (Are et al., 2002; Day et al., 2011; Turner, 2009; Jafari et al. 2019). As a result, discussion hereafter is focused on undrained shear strength.

4. Undrained shear strength

The undrained shear strength mobilized on a full-scale failure surface (i.e., surface on which sliding occurs; see Fig. 3) in the field can be significantly different from the strength measured by in-situ or laboratory tests for the following reasons:

1. A shear test does not typically duplicate the modes of shear along a slip surface in the field (e.g. compression vs. extension);
2. The field undrained strength may be mobilized over a much longer period than in laboratory and in-situ tests;
3. Progressive failure or strain softening of the soil, which is the decrease in shear strength after the peak strength with further strain; and

4. Soil disturbance is a factor only in these tests.

This section provides a background on the four mechanisms and describes the corrections for shear testing. On a single failure surface (see Fig. 4), segments are subjected to different modes of shear. In particular, the surface of sliding in a soft clay beneath an embankment may include segments subjected to compressive, simple, and extension shear. The mobilized shear strength for the embankment in Fig. 4 is a combination of the three modes of shear stress. Quantifying the strength in each mode is important because the compression mode of shear leads to higher undrained shear strength than soil extension (tension), as compression takes advantage of the resistance of the natural soil structure. A single laboratory or in-situ testing device or procedure cannot duplicate all the modes of shear along a full-scale slip surface in the field. Each type of test corresponds mainly to one mode of shear. Moreover, the mode of shear for some tests, such as the horizontal shearing on a vertical surface that occurs in the field vane test, *does not correspond to any actual failure condition in the field*. In fact, a correction factor formed from failed embankment case histories is applied to reduce the field vane measurement to match the shear strength along the failure surface (Mesri and Huvaj, 2007). In comparison, the cone penetrometer is typically benchmarked to laboratory undrained shear strength experiments, including triaxial compression and extension and direct simple shear (Stark and Delashaw, 1990; Kulhawy and Mayne, 1990; Yu and Mitchell, 1998; Mesri and Shahien, 2003; Mayne, 2007). The velocity profile generated from an advancing storm surge accompanied by waves imparts a bed shear stress upon the marsh surface. When the surge recedes, it imparts the bed shear stress in the opposite direction. Thus, the flooding and ebbing of water is bidirectional and is likely represented by the direct simple shear mode of failure, if the wetland moves laterally. The primary failure plane for uprooting of a marsh typically lies below the root mat (Barras et al., 2010; Howes et al., 2010). However, the storm surge and wave interaction with vegetation is complex (Zhao and Chen, 2013) and the loading from small-scale eddies could also uproot the vegetation (Howes et al., 2010). In this case, a triaxial extension mode of shear is more representative. The flexibility of the CPT allows it to be calibrated to these failure modes, especially if high-quality undisturbed samples can be collected from the field. For marsh edge erosion due to

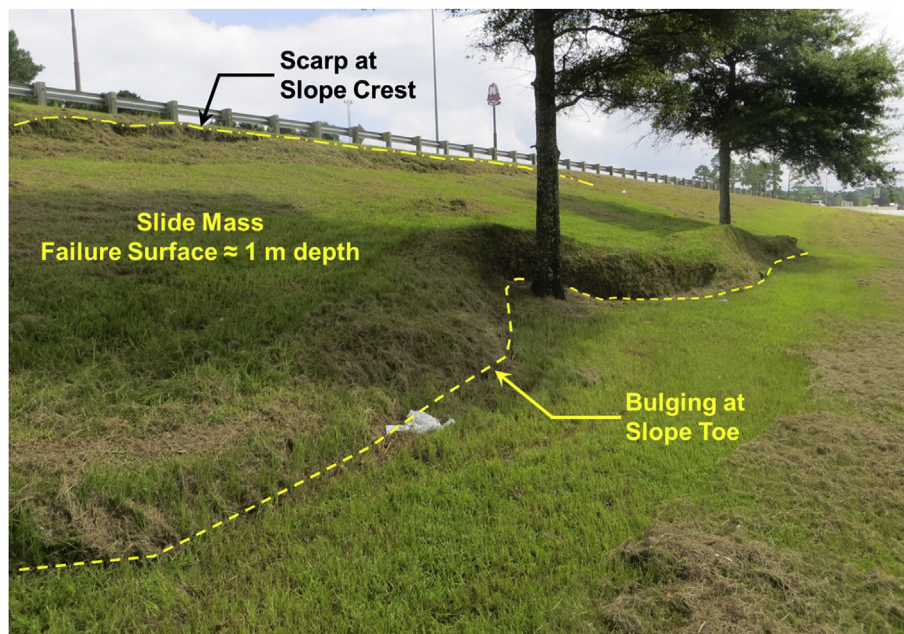


Fig. 3. Shallow slope failure at a Louisiana highway embankment where the sliding surface is 1 m depth. The scarp or cracks at the slope crest and soil bulging at the slope toe are common characteristics of a slope failure (photo courtesy of Jack Cadigan).

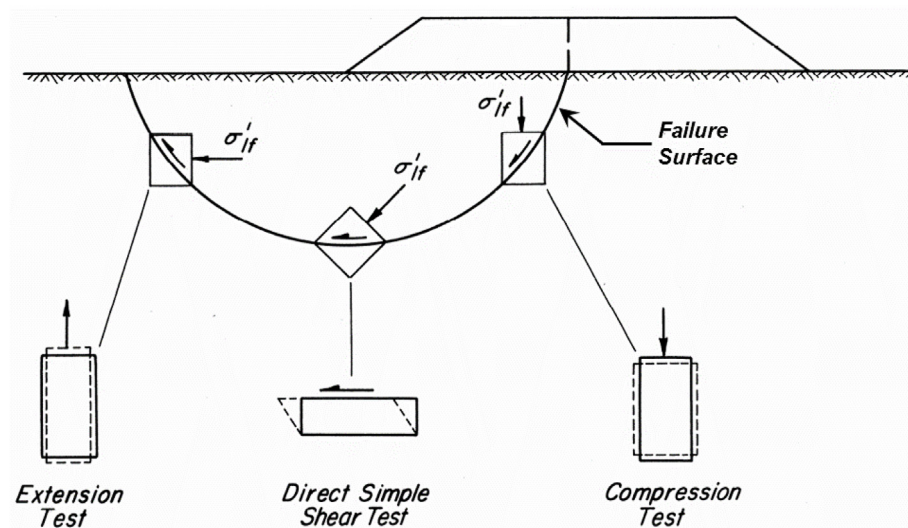


Fig. 4. Relevance of laboratory shear tests to modes of shear on a surface of sliding in the field (modified from Terzaghi et al., 1996).

undercutting, waves impact the vertical soil scarp in the horizontal direction. This is best represented by triaxial compression but rotated in the horizontal direction. In-situ test methods that directly measure lateral stiffness of soils include the flat plate dilatometer (ASTM D6635; Marchetti, 1980; Schmertmann, 1986) and pressure meter (ASTM D4719; Menard 1975; Briaud, 1992).

Mobilization of the undrained shear strength of clays under embankment, footing, or excavation loading usually occurs over a period of weeks. In laboratory and in-situ undrained shear tests, the clay is brought to yield within a few seconds or minutes (as in field vane, cone penetrometer, and unconfined compression tests), or hours (as in triaxial compression, triaxial extension, and direct simple shear tests). The mobilized undrained shear strength of clays and silts decreases as the time to failure increases. Thus, the undrained shear strength measured by in-situ or laboratory tests in minutes to hours can be considerably greater than the strength mobilized in field instabilities over a much longer time. The hydrograph for Hurricane Katrina spanned approximately 36 h (Jafari et al., 2015), and the Mississippi River flood of 2011 lasted over two months, which may have resulted in long term wetland loading on the scale of days-months.

Progressive yielding refers to the non-uniform mobilization of shear strength along a potential failure surface, i.e., shear strength is not the same along the failure surface in Figs. 2 and 3. For example, under an embankment loading, the compression segment of the slip surface is strained beyond its peak strength and loses resistance before the strengths along the horizontal slip surface (direct simple shear in Fig. 4) and the extension segment are fully mobilized. Thus, non-uniform strains and unequal strains to yield for different modes of shear, separately or together, lead to progressive yielding on the surfaces of sliding in the field. When a failure develops such as in Fig. 3, the average shear strength mobilized along the surface of sliding may be significantly less than the average of the peak strengths of the modes of shear on that surface. The likelihood of progressive failure is especially great for highly structured, strain-softening clays and silts. Progressive yielding may be present in construction of containment dikes for marsh creation cells because of the formation of a circular failure surface. The applicability of progressive yielding in wetlands is unknown because of the lack of field observations documenting wetland failure, though remote sensing tools such as InSAR may aid wetland failure observations (Wdowinski and Hong, 2015). Nevertheless, wetland soils with roots likely exhibit strain hardening, where the soil and root matrix strengthens with increasing strain (Cofie, 2001) so progressive yield may be less likely than soft homogenous clay deposits.

All specimens of natural soil deposits tested in laboratory shear

devices experience disturbance. The disturbance likely occurs during sampling and handling in the field, during transit to the laboratory, and during laboratory storage and trimming of specimens for the tests. The most serious mechanism of disturbance is shear distortion of the natural soil structure produced by displacement of the soil during conventional core sampling and handling. Other mechanisms of disturbance, which operate especially during long storage periods, are redistribution of water from the outside to the relatively less disturbed inside of the sample that is eventually tested, and chemical changes including oxidation (Terzaghi et al., 1996). Specimen disturbance leads to highly variable laboratory undrained shear strength measurements. For example, the unconfined compression undrained shear strengths s_{uo} (UC) of low quality samples can be less than 50% of high quality samples (Terzaghi et al., 1996). Wetland cores taken using traditional compressive sampling techniques such as vibracoring undergo changes in in-situ properties such as an increase in bulk density when the sample is taken (volume compression) as well as during transportation of samples from the field to the lab (Kuecher, 1994). As a result, the quality of sampling in wetland cores will dramatically affect the measured shear strength if laboratory experiments are performed.

Beyond the substantial time commitment required for analyzing field cores, measurement errors are pervasive due to variations in operation, type, and dimension of the coring device; compression of the sediment when taking the core and/or when extracting the core from the core tube; imprecise sectioning of the core into known volumes, variation in drying and furnace temperatures, and presence of salts that precipitate when the pore water is evaporated from the sample (Morris et al. 2002). In-situ tests that rapidly evaluate wetland soil properties represent an excellent opportunity to eliminate these drawbacks, strategically select the number and location of core samples, and reduce the impact of sample disturbance. Nevertheless, soil disturbance also occurs to some degree during field vane and cone penetrometer tests because the insertion of the vane and cone tip into soft clays causes displacements and changes in stress that disrupt the natural structure of the soil. For example, disturbance increases and the undrained strength from field vanes decreases as the vane blade thickness increases (La Rochelle et al., 1973). Although disturbance cannot be eliminated completely, its adverse effect on the applicability of the test results can be minimized by standardization of equipment (e.g., vane stem diameter and blade thickness, cone tip diameter and angle) and operation (e.g., rotation and penetration rates). The wetland roots act like reinforcement during shearing, thereby increasing the shear strength. The vane and cone penetrometer can drag and/or cut through the roots.

Before the undrained shear strength measured in shear tests is used

in a stability or foundation design analysis, it must be corrected for the effects of mode of shear, time to failure, progressive yielding, and soil disturbance, or it must be calibrated against the strength mobilized in full-scale field failures (Terzaghi et al., 1996; Mesri and Huvaj, 2007). Similarly, for comparing wetland shear strengths, it is critical to reconcile these measurements into a common reference frame in order to draw conclusions regarding impacts of nutrients and sediment dynamics. This could be accomplished by converting the measured in-situ and laboratory s_u to a mobilized $s_{u,m}$, the shear strength developed in resistance to an applied load. The most practical approach is to calibrate in-situ or laboratory test values against undrained shear strengths back-calculated from actual failures, e.g., marsh erosion after a hurricane as reported in Howe et al. (2010). Alternatively, a comprehensive field campaign can be performed with all available shear strength instruments and correlations can be developed that relate one instrument's results to another. For example, the cone penetrometer and standard penetrometer tests are indirectly correlated through the drained friction angle of sands (Terzaghi et al., 1996). Large block samples can also be taken for high quality laboratory shear strength testing and comparison to the field methods, as was accomplished by Mesri et al. (1997) for compressibility testing of peats located in Wisconsin.

5. IN-SITU and laboratory strength measurements

The usefulness of a shear test for obtaining undrained shear strength is measured by its simplicity, the reproducibility of its results, and whether the values it yields are comparable to other in-situ shear strength measurement techniques. The most common methods of obtaining or directly measuring the undrained shear strength are field vane (FV) shear tests and cone penetrometer tests (CPTs) along with laboratory unconfined compression (UC), triaxial compression (TC), triaxial extension (TE), torsional ring shear testing, and direct simple shear (DSS) tests. Although most in-situ and laboratory shear devices test a relatively small element of soil, this limitation is rarely a serious problem in the measurement of the undrained shear strength of homogenous soft clays. In contrast, wetland soils can contain variable percentages of soil types, roots, stems, and shells that affect the measured shear strength. For example, the soil samples in Fig. 5 demonstrate the difference between homogenous soft clays (Fig. 5(a)) and organic clays with roots (Fig. 5(b)). In the case of organic clays, testing a larger soil volume provides a more representative shear strength. In addition, testing a small sample size, such as by a torvane, can be significantly influenced by individual roots that may suggest higher strengths than the global soil matrix. For the soils in Fig. 5, cone penetrometer and field vane measurements (blade dimensions of 130 mm by 65 mm) provided similar undrained shear strengths for the homogenous soft clay. However, the field vane was not able to measure a strength in the organic clay because the torque meter maxed out before failure. This observation highlights the possible limitations of the field vane in soils containing plant roots and rhizomes. Discussion of the in-

Table 1

Consistency of clay in terms of undrained shear strength measured by unconfined compressive strength (after Terzaghi et al., 1996).

Consistency	Undrained Shear strength (kPa)
Very soft	< 12
Soft	25–50
Medium	50–100
Stiff	100–200
Very stiff	200–400
Hard	> 400 kPa

situ test methods in relation to wetland soils is provided in subsequent sections.

The consistency of clays and other cohesive soils is usually described as soft, medium, stiff, or hard. Table 1 relates various degrees of consistency to values of undrained shear strength based on the laboratory unconfined compressive strength. Very soft clays are characterized by shear strengths less than ~12 kPa, e.g., surficial normally-consolidated soft clays and peats along with recently deposited marine sediments. In most cases, this low shear strength is a byproduct of a low effective stress (Mesri and Aljouni, 2007; Mesri and Huvaj, 2007), e.g., near surface deposits as depicted in Fig. 1. Strengths of very soft clays are difficult to quantify with standard geotechnical field and laboratory equipment because of the resolution of the load sensors. CPT tip modifications to increase the surface area and hence tip resistance sensitivity of a CPT may be accomplished by modifying the traditional conical shape of the cone tip to a spherical ball or T-bar (Yafate et al., 2009; DeJong et al., 2010). Moreover, the lowest feasible shear strength for soft clays occurs under the remolded case, i.e., process of kneading the soil until it significantly softens. Shear strengths on the order of ~1 kPa are possible but special laboratory equipment (viscometer, rheometer, and fall cone apparatus) are needed. This illustrates that geotechnical instruments can be limited in making accurate measurements at very low shear strengths, which are relevant for wetland soils.

5.1. Vane tests

The vane shear test and its use for measurement of wetland soil strength is described herein to provide context and reservations about use of this technique in wetland soils. The field vane apparatus was designed for soft homogenous clay deposits and the results are typically used for designing earthworks and foundations (Terzaghi et al., 1996; Carlson, 1948; Cadling and Odenstad, 1950). ASTM D2573 (2015) provides the standard test method, including vane apparatus, calibration of torque device, and procedure. The ASTM standard indicates that the vane shear test is applicable to saturated fine-grained soils (clays and silts) or other saturated fine-grained geomaterials, such as mine tailings and organic muck, for undrained strengths of less than 200 kPa (4000 psf). The vane shear test consists of placing a four-bladed vane in the intact soil and rotating it at a rate of 6°/minute from the surface to

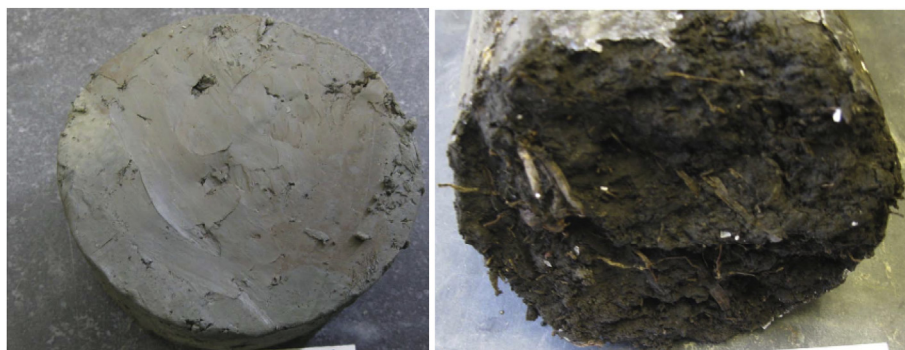


Fig. 5. (a) Homogenous high plasticity clay, and (b) organic clay.

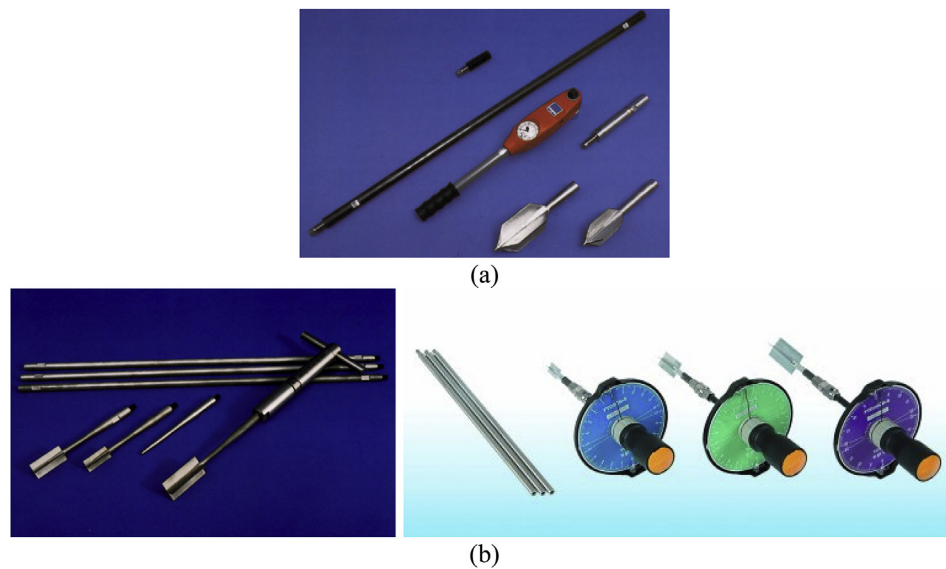


Fig. 6. Examples of (a) field and (b) hand-held vanes (photos courtesy of Geonor and Seiken).

determine the torque required to shear a cylindrical surface with the vane. This torque is then converted to a unit shearing resistance of the failure surface by limit equilibrium analysis (Eq. (4)).

$$Su(FV) = \frac{T}{\frac{\pi D^3}{1} + \frac{\pi D^3}{6}} \quad (4)$$

where T is the maximum value of measured torque (N-m), D is the diameter of the vane (m), and the height of the blade (D) is equal to 2D. The subscript 1 (πD^3) refers to the surface area sheared along the vertical plane of the cylinder, while subscript 2 ($\pi D^3/6$) corresponds to shearing on the top and bottom of the cylinder created by the rotating vane.

ASTM D2573 (2018) also applies to hand-held vane shear tests typically performed at shallow depths in coastal marshes. The major difference between the field vane and hand-held vane is the blade dimensions, e.g., 35–100 mm in height and 12.7–25.4 mm in diameter, respectively (see Fig. 6). The ASTM standard indicates that hand-held equipment may be less accurate because it may be more difficult to maintain vane/rod stability and verticality. Moreover, the quality of the result produced by this standard is dependent on the competence of the personnel performing it. For example, the rate of vane rotation greatly affects measured shear strengths (Schlue et al., 2010), and may vary by operator. ASTM D4648 (2016) recommends that the hand-held vane test be conducted in fine-grained, predominately clay soils with an undrained shear strength less than 100 kPa. The vane test is not recommended in any soil that permits drainage or dilates during the test

period, such as stiff clays, sands or sandy silts, or soils where stones, large roots, or shells are encountered by the vane in such a manner as to influence the results. In addition, insertion of the vane cuts roots in the soil, creating an altered soil structure due to the separation of the tensile reinforcement (roots) within the soil matrix.

Many wetland studies of shear strength leveraged the use of hand-held vane device (Turner, 2011; Howes et al., 2010; Wilson et al., 2012; Chen et al., 2012; McClenachan et al., 2013; Wigand et al., 2014; Graham and Mendelssohn, 2014; Bentley et al., 2015a,b; Leonardi et al., 2016; Lin et al., 2016; Ameen et al., 2017; Turner et al., 2018). Howes et al. (2010) investigated strength of low and high salinity wetlands in Breton Sound, LA. Wilson et al. (2012) focused on the effect of crab bioturbation along tidal creeks in Camp Romaine, SC. McClenachan et al. (2013) and Lin et al. (2016) reported the changes in shear strength due to oiling of salt marsh in Barataria Bay, LA. Chen et al. (2012) and Leonardi et al. (2016) measured strengths in Beaulieu Estuary, England and Plum Island, MA, respectively, to better formulate marsh edge erosion relationships with wave power. Wigand et al. (2014), Graham and Mendelssohn (2014), Turner (2011), and Turner et al. (2018) studied the influences of biogeochemical processes (added nutrients) on wetland strength in Jamaica Bay, NY, north Lake Pontchartrain, Terrebonne Bay, and Hammond, LA, respectively. Bentley et al. (2015) and Ameen et al. (2017) measured wetland strength of Breton Sound and Barataria Bay along with an artificial crevasse splay at West Bay, LA, respectively, to address potential feedback wetland responses to hydrology and geomorphology. Table 2 summarizes the references, location, and methods from these studies.

Table 2
Summary of hand-held vane strength measurements in wetlands.

Reference	Vane Device	Location
Turner (2011)	Dunham E-290	Salt marsh near Cocodrie, LA, USA
Howes et al. (2010)	Seiken field vane Wykeham Farrance lab vane	Breton Sound, LA, USA
Leonardi et al. (2016)	Hand Vane	Plum Island Sound, MA, USA
Bentley et al. (2015)	Geonor Hand Vane	Barataria and Breton Sound, LA USA
Wigand et al. (2014)	Hand vane	Jamaica Bay, NY, USA
McClenachan et al. (2013)	Dunham E-290	Bay Batiste, Barataria Bay, LA, USA
Turner et al. (2018)	Dunham E-290	Four-Mile Marsh, Ponchatoula, LA, USA
Wilson et al. (2012)	Seiken shear vane	Cape Romain, South Carolina, USA
Graham and Mendelssohn (2014)	5 cm long shear vane with torque gage	Low salinity marsh, Lake Pontchartrain LA USA
Lin et al. (2016)	5 cm long shear vane with torque gage	Barataria Bay, LA, USA
Wigand et al. (2018)	Hand vane	Plum Island, MA

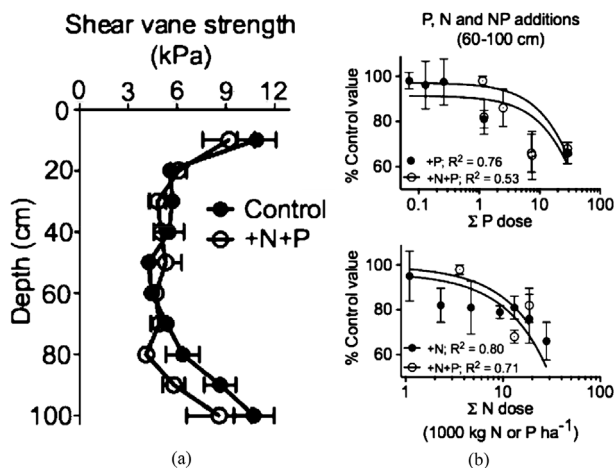


Fig. 7. (a) The shear vane strength (kilopascal; $\mu \pm 1$ SE) for replicated control and +N + P treatment plots for the 10 cm–100 cm soil depth; (b) The average shear vane strength at 60- to 100-cm soil depth as a percent of the value in the control plots versus the cumulative N and P load (Σ 1000 kg ha⁻¹) for plots fertilized with +P or with +N + P (upper panel) or plots fertilized with +N and +P + N (lower panel) (figures from Turner, 2011).

The following discussion provide examples from these studies that further detail the implementation of shear strength measurements in wetlands from the hand-held vane device and how the results were interpreted.

Fig. 7 shows shear strength results that Turner (2011) measured by a Dunham E-290 hand-held vane tester (blade diameter = 25.4 mm, height = 50.8 mm). Measurements were obtained every 10 cm from control and nutrient enriched plots on a 1 m profile to investigate changes in strength from control and nutrient enriched plots. Turner (2011) indicates that in each plot three to six vertical profiles were obtained, i.e. the mean and standard error ($\mu \pm 1$ SE) were calculated using 3 to 6 measurements at each 10 cm depth increment. For statistical analyses, Turner (2011) used a one-way analysis of variance with a Tukey's multiple comparisons test to determine whether there were significant differences in soil strength between the control and triplicate treatment plots and among different kinds of treatment plots ($p < 0.05$). Turner (2011) indicates that there was no difference in the shear vane strength between control and +N + P treatments in the upper soil profile (20–50 cm), but the soil strength was reduced by about 21% in the 60 cm to 100 -cm soil layer of the +N + P treatment plots. If the belowground biomass is typically within the first 30 cm from the surface, it is unclear why and how nutrients could cause lower shear strengths in the 60 cm–100 cm interval, though Turner (2011) indicate that the soil below the 60 cm depth is at least 100 years old and contains organic matter formed prior to the occurrence of major water quality changes. Turner (2011) uses the change in tensile strength of canvas strips placed in fertilized and control plots to imply that nutrient amendment also caused significantly higher decomposition down to 60 cm. However, the change in water content and organic matter with depth could help better elucidate if increased decomposition rates was in fact occurring and if it was changing the soil structure with depth that in turn could affect the shear strength.

Fig. 7(a) shows varying mean and SE shear strength with depth. Average strengths of at least 9 kPa were observed at the 10 cm depth likely because of the added reinforcement and interaction of the blade with roots. The relatively higher SE bars at this depth may correspond to the greater root biomass, which can mean higher strengths and more variability because of the likelihood the vane interacts with the interwoven network of roots and rhizome when inserting and then rotating the blade during shearing. The shear strength decreases to a minimum beyond the root mat before increasing again as the vane approaches a stiffer grey clay layer. This trend in the strength profile is similar to

measurements by Jafari et al. (2019) in Terrebonne Bay, near Cocodrie, LA. Establishing the strength loss or gain from nutrient loadings in Fig. 7(a) is not clear because of the SE values. SE independently does not provide much information, but it can be used to estimate the confidence interval of the data. For example, $\mu \sim 9.1$ kPa and $SE \sim 1.5$ kPa at a depth of 10 cm for the N + P plots and $\mu \sim 10.9$ kPa and $SE \sim 1.3$ kPa for the control plots. This indicates that there is a 68.2% likelihood that the actual shear strength of the wetland is within 1.5 kPa or 1.3 kPa of the reported means, respectively. When the ± 1 SE bars overlap, there is no significant difference in the mean shear strengths. This is more evident if the ± 2 SE bars are plotted because it represents a 95% confidence interval ($p < 0.05$). In Fig. 7(a), the control and nutrient enriched plots overlap except at depths of 80 cm and 90 cm, i.e., sufficient evidence is not available to ascertain conclusive effects of nutrients on shear strength. Although the ± 1 SE bars do not overlap at 80 cm and 90 cm, the strengths only vary by 2–3 kPa, which is negligible in geotechnical engineering because a difference in behavior is not observable. The main function of the SE is to facilitate construction of the 95% and 99% confidence intervals, which can supplement statistical significance testing and indicate the range within which the true mean or difference between means may be found. Engineers predominantly use standard deviation (SD) and coefficient of variation (COV) for quantifying the uncertainty or dispersion in the data, which is subsequently used in reliability analyses to predict the probability of failure of infrastructure. However, statistical methods are common tools in wetland ecology studies in order to make inferences. Thus, when the SE bars do not overlap, does this signify a statistical difference in strength? More importantly, does it represent an ecologically significant difference? Engineers often refer to “engineering judgement” or a sense of proportion (Peck, 1967) when deciding what constitutes a significant change in strength values. In other words, does the soil behave in a remarkably different manner? In the case of Fig. 7(a) for depths of 80 cm and 90 cm, the difference in strength between control and enriched plots is approximately 3 kPa, which may be within the uncertainty of the vane device. More importantly, both measurements reflect a soft soil with low shear strength (< 10 kPa) that behaves similar to a viscous liquid.

Fig. 7(b) suggests that the shear strength decreases with increasing dosage of nitrogen and phosphorus nutrients (+N, +P, and N + P). In particular, the ordinate axis is reported as % control value, which corresponds to the ratio of nutrient strength divided by the control strength. The upper panel shows +P and +N + P strength ratio as a function of cumulative P dosage, while the lower panel shows the +N and +N + P strength ratio as a function of cumulative N dosage. The % control value for the lower panel Σ N is approximately equal from 2000 to 20,000 cumulative N kg/ha/yr dosage. The R^2 value for semi-log best fit trend lines suggest a trend exists, but the data does not visually follow the trend line. For the Σ N dosage, the data points fall at approximately 80% control. The +P and +N + P visually show more effect but at the extremely high doses, which are ecologically rare. Moreover, the differences in shear strength in the deep profile (60 cm–100 cm) is not ecologically important in response to natural and human caused stressors, compared to the first 30 cm which encapsulates the belowground biomass.

The debate between statistical significance, ecological significance, and engineering judgement is also observed in Fig. 8, which shows overall higher strengths at Hammond, LA freshwater marsh than the LA salt marshes in Fig. 7. The general soil strength profile also differs from Fig. 7 and subsequent figures in that the lower depths are greater strength than near the surface (depth < 50 cm). Additional information about the soil and vegetation properties for the 0–100 cm profile is needed to better explain the contrasting strength profile. In Fig. 8, the ± 1 SE bars overlap for all depths except at the surface and 80 cm, which suggests no significant difference in the strengths between the control and transition zone. A visual break in strength appears below the root mat, but the high SE on the order of 10 kPa for $n = 5$ samples

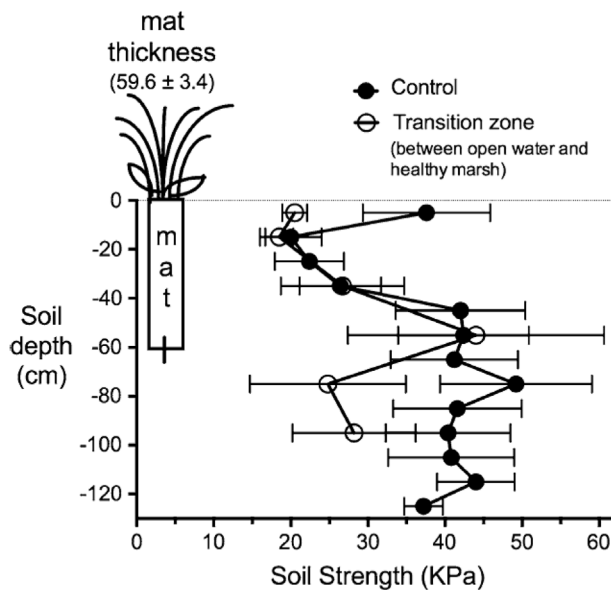


Fig. 8. The average soil strength (kPa) for the control areas (every 10 cm) and the transition zone (every 20 cm) at the edge of the open water, to 50 m inland. The average thickness (cm; 1 ± 1 SE) of the mat sampled 3 September 2012 when the Hurricane Isaac flood waters were 1.5–2.0 m over the marsh (from Turner et al., 2018).

needs to be reduced or an alternative technique beyond the hand-held vane that is repeatable and accurate should be used to elucidate any influence of the sewage discharge.

Showing the individual vane measurements along with μ and SD for each increment and study variable would be beneficial and practical for drawing conclusions on soil strength. Moreover, 3 to 6 measurements may not be a sufficient number of measurements to form conclusions, especially if the coefficient of variation (CV) for undrained shear strengths reported in geotechnical engineering literature ranges from 13% to 40% (Harr, 1984; Kulhawy, 1992; Lacasse and Nadim, 1997; Duncan, 2000). Assuming a CV of 40% (likely considering root interactions with the small vane blade) and $\mu = 8$ kPa for 6 vane measurements, the corresponding SD and SE are 3.2 kPa and 1.3 kPa, respectively. The high CV, low strengths, and limited sample size results in an anticipated shear strength of 5.5 kPa–10.5 kPa at a 95% confidence interval. As a result, further studies are needed to define the CV of the hand-held vane for wetland soils. Moreover, scientific journals are providing options to publish datasets as supplemental materials. This is highly recommended so other scientists and engineers can leverage these measurements for further uncertainty analyses.

Wigand et al. (2018) conducted hand-held vane strength measurements at six tidal creeks located in the Plum Island estuary, Massachusetts (Deegan et al., 2007, 2012; Johnson et al., 2016). In particular, Wigand et al. (2018) investigated the vertical profile and horizontal variation of shear strength, starting from the tidal creek and moving inland to the interface of the high marsh. At each habitat location, two reference creeks are used to compare against long (9 years) and one reference creek with short-term (4 years) nutrient enrichment treatments. In contrast to other nutrient studies (e.g., Turner, 2011; Graham and Mendelssohn, 2014), the nutrient loading in this study leveraged tidal flooding that occurred twice daily, which was 70–100 $\mu\text{mol/L}$ NO_3 (as NaNO_3) and 10–15 times greater than Plum Island Sound background levels (Johnson et al., 2016). Nutrient loading rates to creek banks are close to 1000 $\text{g N/m}^2/\text{yr}$ (see Day et al., 2018). The two dominant marsh landscapes of creek (~2–3 m wide) and high marsh are characterized by tall *Spartina alterniflora* and *Spartina patens*, respectively. The interface zone is ~1 m wide and consists mostly of stunted *S. alterniflora*, along with *S. patens* and *D. spicata*. These three habitat

locations were tested to evaluate horizontal variation in shear strength.

Wigand et al. (2018) set four transects in each habitat (creek, interface, high marsh) for the long-term enriched and corresponding reference creeks (24 total vertical profiles) and eight (8) transects in each habitat for the short-term and corresponding reference (24 total vertical profiles). They also conducted hand-held vane tests (20 mm blade width by 40 mm height) within 2 h of the low tide to better facilitate a comparison, likely attributed to soil water content and water loading. Moreover, the vane shear strengths were averaged between 10 and 30 cm, 40–60 cm, and 70–90 cm to examine for differences in shear strength with depth (vertically), among habitats (horizontally), and between nutrient treatments. To more closely examine the soil shear strength associated with the *S. alterniflora* active rooting (10–30 cm) and sub-rooting (40–60 cm) depths, Wigand et al. (2018) calculated a vertical shear strength differential between these intervals for the creek bank and interface zones. For each location sampled along the transects in these two zones, the 10–30 cm depth soil shear strength was subtracted from the 40–60 cm soil shear strength to calculate a vertical differential (see Fig. 2 in Wigand et al., 2018). The vertical shear strength differential suggested that the 10–30 cm root zone is weaker at the interface of enriched creeks. This is also evident in the contrast in white and dark grey colors in Fig. 9 corresponding to the interface of enriched creeks. Fig. 9 also shows the vertical and horizontal patterns of shear strength in the reference and nutrient treated plots. For the short-term creeks, the only visual difference corresponds to the interface and high marsh. The enriched high marsh suggests lower strengths at the 60–90 cm interval, while a constant strength is visually observed for the high marsh reference. It is unknown why the soils are weaker at the 60–90 cm interval, but it could be attributed to heterogeneity in soil stratigraphy. The impact of nutrients at that depth and inland location seems less likely if cohesive sediments are present (Deegan et al., 2012). In contrast, the long-term enriched creek strengths are visually higher than the reference creeks, except a slight decrease at the 10–30 cm interval for interface and creekbank locations. The formation of cracks and slumping in the enriched marshes were observed during this long-term study (Deegan et al., 2012; Wigand et al., 2018). This represents an intriguing geotechnical problem that is similar to stream banks, levees, and dams, where cyclic loading and unloading from the water along with flow into and out of the bank can cause a slope failure. Further integrated geotechnical numerical, laboratory, and field investigations are warranted to better understand how the mechanical response of the creekbank are affected by the tidal cycle.

The study also used linear mixed effects models to statistically analyze the effects of nutrient enrichment, habitat, and depth on shear strength. Discussion of this statistical model is beyond the intention of the review, but it is emphasized that a consistent approach to evaluating the data is necessary. In particular, analysis of variance (ANOVA) is a common method used to infer if statistical differences exist in shear strength, among many other ecological parameters. However, does a statistically significant inference actually relate to a practical or observable difference in shear strength? From an engineering perspective, shear strengths between control and treatment could be sufficiently close that the behavior is essentially the same. Answering this question is paramount to understanding the role of shear strength in wetland ecology. A discussion is provided further into the review where the shear strength from the marsh edge, interior marsh, and mudflat are compared to demonstrate an observable difference in shear strength that is also ecologically significant.

The raw data in Wigand et al. (2018) is plotted in Fig. 10 in terms of the average shear vane strength with ± 1 SE, which is similar to Figs. 7(a) and Fig. 8. Fig. 10 shows the short and long-term nutrient enrichment and reference results, where each data series contains a different symbol but the reference sites and nutrient-enriched sites consist of the same colors to facilitate visual comparison with the SE. For example, the creek reference and nutrient enriched strengths overlap along the entire vertical profile, especially in the first 30 cm.

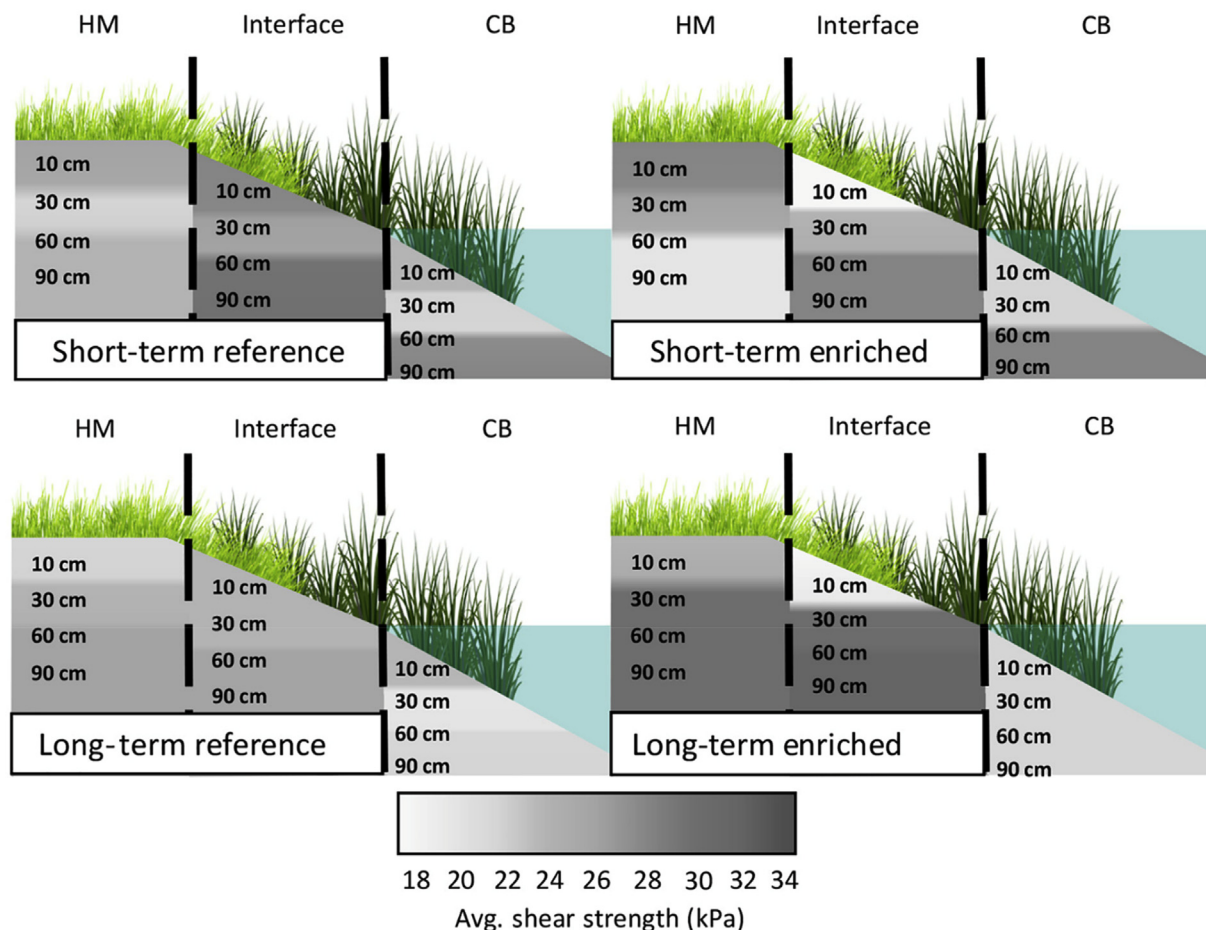


Fig. 9. Visual representation of average shear strengths for high marsh (HM), interface, and creek bank (CB) vegetation zones at depth intervals of 10–30, 40–60, and 70–90 cm for the short- and long-term enrichment and reference creeks (figure from [Wigand et al., 2018](#)).

This suggests that the nutrient enrichment did not affect the root and underlying soil strengths, although [Deegan et al. \(2012\)](#) show that belowground biomass does significantly vary in the creekbank, and more importantly that there is significant fracturing at the creekbank in the nutrient treated marshes. For the interface zone, there was a statistically significant difference in strength at the 10 cm depth, between the nutrient enriched strength of ~18 kPa and reference (~26 kPa and ~38 kPa). The high marsh references show similar behavior and magnitude of strength, but the nutrient enriched transects exhibited contrasting behaviors. For example, the short-term values are higher near the surface but are lower than the long-term transect below 40 cm. The reference strengths for interface and high marsh zones are within 20–30 kPa, while the creek reference strengths are slightly less than 20 kPa. This may indicate the creek is more susceptible to fracturing than the high marsh, although the high marsh may transition to lower strengths as the tidal creek erodes. The comparison of shear strength by the hand-held vane between Plum Island and Louisiana is captured by [Fig. 7\(a\)](#) for Louisiana and [Fig. 10](#) for Plum Island. In particular, the strengths in Louisiana are less than 15 kPa, while [Fig. 10](#) indicates that the shear strengths measured in Massachusetts were all above 20 kPa. This alludes to regional contrasts in shear strength across the U.S.

The variability in the hand-held vane shear measurements, due to inconsistent operator speed and shearing zone not being representative of surrounding root-soil structure, is of practical interest in engineering because they provide an indication of the repeatability (precision) of the instrument ([Merrifield, 1980](#); [Ding and Loehr, 2019](#)). Because [Wigand et al. \(2018\)](#) reported the sample number and SE, the standard deviation was back-calculated by the authors for nutrient-enriched and reference marsh landscapes (creek, interface, and high marsh). For

example, [Fig. 11](#) clearly indicates that the SD varies with depth, from approximately 5 kPa–15 kPa. The lowest SD of 5 kPa is observed at the interface zone for the long-term enrichment, which corresponds to a shear strength of ~26 kPa. This SD is likely the lowest value achievable. For example, the average SDs for the short-term reference were 10.7 kPa, 8.2 kPa, and 9.8 kPa for the creek, interface, and high marsh, respectively, while the average SDs for the nutrient-enriched transects were 10.2 kPa, 8.7 kPa, 10.3 kPa for the creek, interface, and high marsh, respectively. The average SDs for the long-term reference were 11.8 kPa, 7.2 kPa, and 7.4 kPa for the creek, interface, and high marsh, respectively, while the average SDs for the nutrient-enriched transects were 10 kPa, 6.2 kPa, 7.2 kPa for the creek, interface, and high marsh, respectively. This suggests that the short-term SDs are similar to the long-term transects, across the three different landscapes and between reference and nutrient-enriched. Using [Figs. 10 and 11](#) and assuming an average shear strength of 25 kPa and SD of 10 kPa for a vertical profile, 95% of the vane data falls between 5 and 45 kPa. Tables in the supplemental materials provide a summary the average, SD, and CV from the [Wigand et al. \(2018\)](#) study. Further testing is required to better constrain the likely range. Nevertheless, [Wigand et al. \(2018\)](#) provides a first indication into the uncertainty in conducting the vane test because of different users, vane equipment, and soil/vegetation/shell heterogeneity, and temporal site conditions.

[Fig. 12](#) shows the relationship between belowground biomass and shear strength measurements in different systems, which is an important relationship to establish as a surrogate for wetland health. [Ameen et al. \(2017\)](#) measured the strength of different vegetation communities in the Mississippi River Birdsfoot delta at the surface of the most densely vegetated area within the quadrat. [Lin et al. \(2016\)](#)

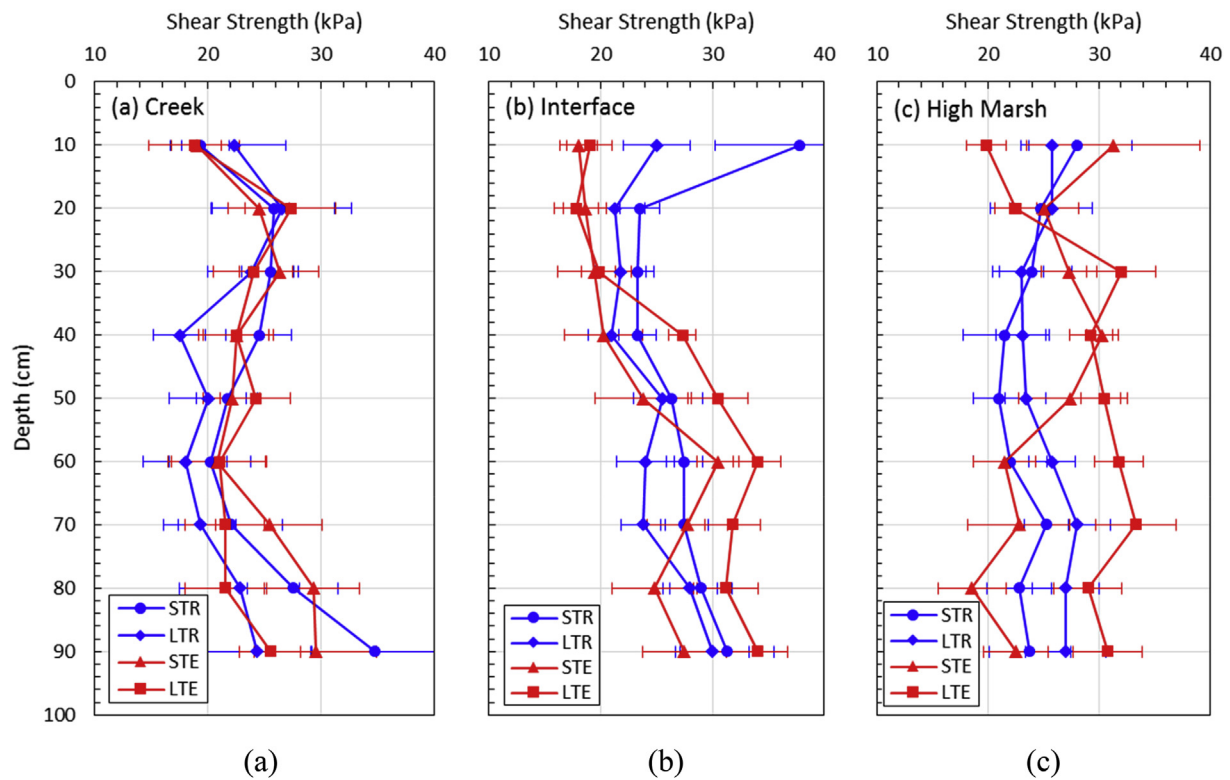


Fig. 10. Vertical shear strength profiles of reference and nutrient enriched wetlands at Plum Island estuary at three marsh landscapes using a shear vane: (a) Creek, (b) Interface, and (c) High marsh (data from Wigand et al., 2018). [STR = short-term reference; LTR = long-term reference; STE = short-term enriched; LTE = long-term enriched; red = enriched; blue = reference; horizontal bars = ± 1 SE]. (For interpretation of the references to color in this figure legend, the reader is referred to the Web version of this article.)

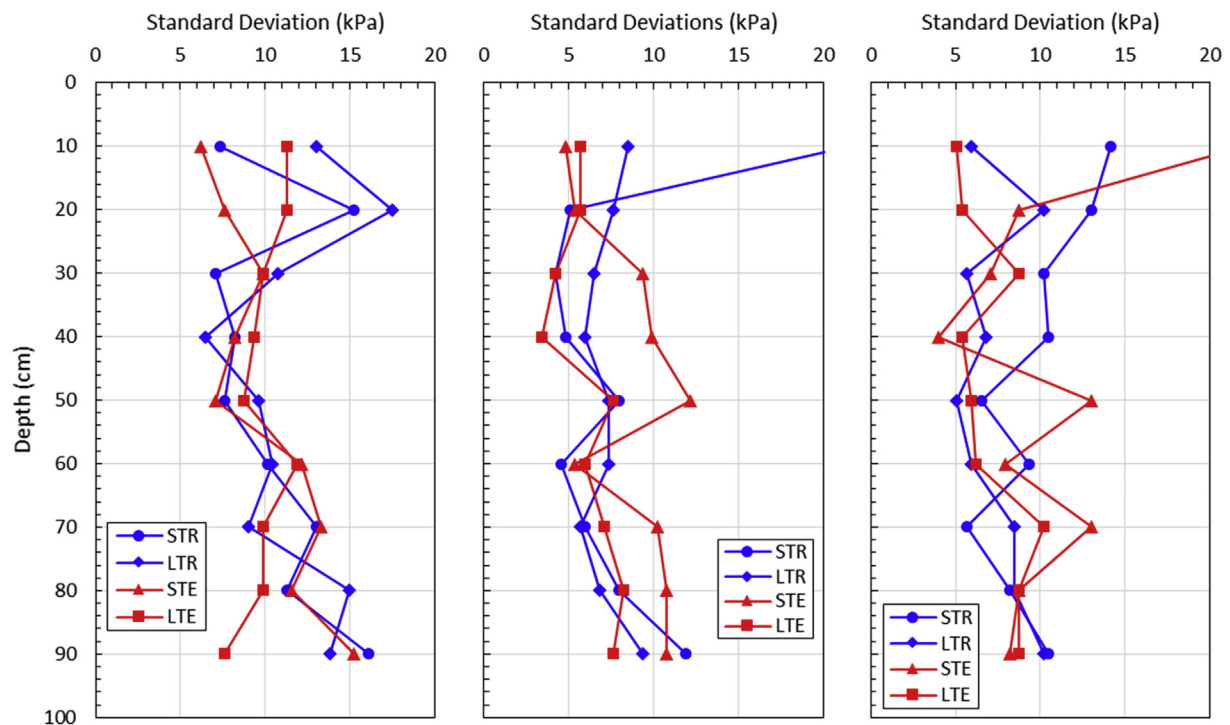


Fig. 11. Standard deviation profiles of hand-held vane measurements for reference and nutrient enriched wetlands at Plum Island estuary at three marsh landscapes: (a) Creek, (b) Interface, and (c) High marsh (calculated from data from Wigand et al., 2018). [STR = short-term reference; LTR = long-term reference; STE = short-term enriched; LTE = long-term enriched; red = enriched; blue = reference]. (For interpretation of the references to color in this figure legend, the reader is referred to the Web version of this article.)

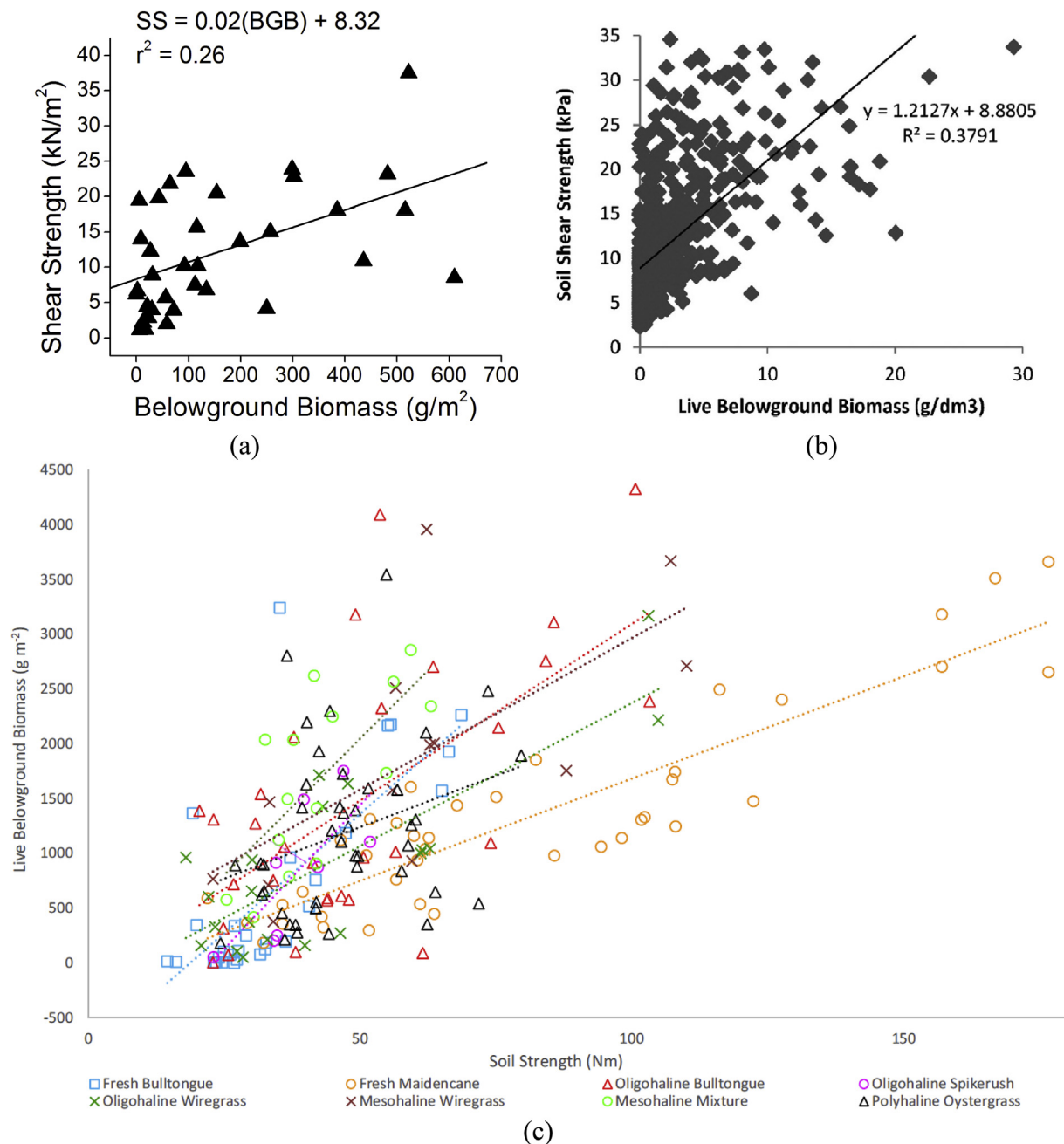


Fig. 12. Relationship between belowground biomass and shear strength: (a) strength at emergent island stations assessed at a mean depth of 11 cm (Ameen et al., 2017); (b) live belowground biomass 24–42 months after Deep Horizon Oil spill (Lin et al., 2016); and (c) live belowground biomass from eight vegetation types and soil resistance measured using the WSST (Sasser et al., 2018).

measured the vane strength at 6 cm intervals to a depth of 36 cm in Barataria Bay, LA in areas impacted by the 2010 Deepwater Horizon oil spill. They report a lower strength at the 6 cm increment compared to the 12 cm depth for heavily oiled wetlands. Lin et al. (2016) indicate the strength decreased from the top to the bottom of the soil profile, i.e., from 22.1 kPa at 6 cm to 5.6 kPa at 36 cm. The SE ranges from 0.27 to 0.6, which is likely attributed to the high number of samples ($n = 126$). Fig. 12(a) and (b) display considerable scatter, with a slight positive correlation. This suggests that belowground biomass is only one of many factors that influence shear strength. Further information could be gleaned from both studies in Fig. 12 if the data was filtered to vegetation community, depth, degree of oiling, and time after the oil spill, where the latter two are specific to Lin et al. (2016). Moreover, both studies suggest that a significant number of soil cores did not produce

any belowground biomass (Lin et al., 2016 = only live; Ameen et al., 2017 = live + dead) even though strengths approached at least 20 kPa and up to 35 kPa. This is in contrast with Sasser et al. (2018) in Fig. 12(c), which reports live belowground biomass near zero for only fresh bulltongue vegetation. The results of both the Ameen et al. (2017) and Lin et al. (2016) studies fall in the extreme lower left corner of Fig. 12(c). Possible explanations for the wide scatter in Fig. 12(a) and (b) at low belowground biomass include: (1) the combined belowground biomass and soil strength varies significantly, and (2) the hand-held vane test is influenced by roots regardless if they are live or dead, i.e., the presence of small roots is sufficient to affect the rotating vane. The small sample volume appears as a major drawback for the hand-held vane test. Reporting the diameter of the roots (live and dead) may help better understand the effect on the vane blade size. The range of

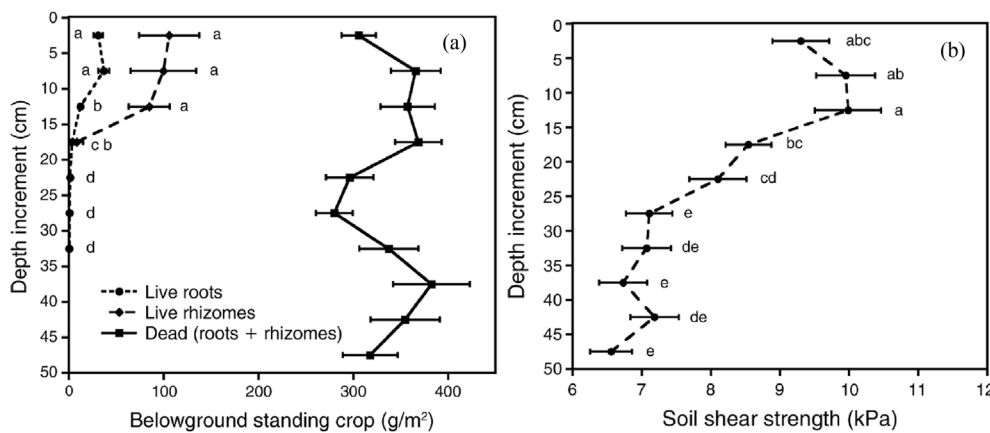


Fig. 13. (a) Live root, live rhizome, and dead standing crop (mean ± 6 SE) with respect to depth (5 cm increments, 0–50 cm; averaged over split-plot herbivory and whole-plot nutrient enrichment treatments). Different letters identify differences among means ($P < 0.05$; Tukey-Kramer multiple comparison test). Where two letters appear at the 15–20 cm depth increment, the letter on the left indicates live roots and the letter on the right live rhizomes. At depths below 20 cm, live rhizomes were not present, and letters indicate living roots. Below 35 cm, living roots were absent; and (b) Soil shear strength (mean ± 6 SE) with respect to depth (5-cm increments, 0–50 cm; averaged over split-plot herbivory and whole-plot nutrient enrichment treatments) (from [Graham and Mendelssohn, 2014](#)).

belowground biomass in [Fig. 12\(b\)](#) is low such that it may represent fluidized wetlands. Compared to measurements in [Fig. 12\(c\)](#) from [Sasser et al. \(2013, 2018\)](#), the belowground biomass less than 50 g/m^2 from [Ameen et al. \(2017\)](#) is on the same order of magnitude of fresh bulltongue, which is a shallow rooted plant with a saturated bulk density near water. [Lin et al. \(2016\)](#) reports live belowground biomass in g/dm^3 . The volume dm^3 (decimeter = 0.1 m) represents the belowground biomass in a plan area along with soil thickness (typically 12 cm). The belowground biomass measurements in [Fig. 12](#) also highlights the need to ensure consistent methods of measuring and reporting belowground biomass in dry weight, including total, live, and dead components.

Instead of using a total belowground biomass from a soil core as in [Fig. 12](#), [Graham and Mendelssohn \(2014\)](#) present live and dead (roots and rhizomes) belowground biomass as a function of depth in [Fig. 13](#). This shows a clear trend of live roots and rhizomes in the upper 15 cm before decreasing to zero at depth of ~ 18 cm. The dead belowground biomass is approximately constant with depth, where the mean ranges from 280 to 370 g/m^2 . When comparing to the hand-held vane shear strengths, a strong visual correlation is observed between the higher strengths of $\sim 10 \text{ kPa}$ in the upper 15 cm and live belowground biomass. Below a depth of 20 cm where only dead belowground biomass is present, the shear strength decreases to approximately 7 kPa , which is only a reduction of 3 kPa . Similar to [Turner \(2011\)](#), the hand-held vane results visually demonstrate the trend of decreasing strength from 15 cm to 30 cm, but it is not clear if the decrease in 3 kPa represents a measurable difference in the wetland strength that can be sensed by the operator of the vane device. [Fig. 13](#) still shows that live belowground biomass plays an active role in shear strength and dead belowground biomass represents lower strength of the organic soils. Further studies similar to [Graham and Mendelssohn \(2014\)](#) are recommended to better understand the biogeochemical processes affecting wetlands, with added information of root diameter and tensile strength along with the application of other test methods, such as the WSST and cone penetrometer.

The hand-held vane test has many advantages when used in homogeneous soft to medium stiff clay deposits, e.g., a quick and simple estimate of the undrained shear resistance of cohesive soils in the field. However, the accuracy of the hand-held vane is reported as 10% for homogenous soils ([Roctest, 2011](#)). [Fig. 14\(a\)](#) shows vane strength data from wetlands in Lower Breton Sound ([Bentley et al., 2015](#)), while [Fig. 14\(b\)](#) shows a comparison of high and low salinity wetlands in Breton Sound ([Howes et al., 2010](#)). These studies show that the hand-held vane method is capable of outlining only the *general trend* in wetland strength with depth. For example, the hand-held vane results show that shear strength increases linearly with depth in [Fig. 12\(a\)](#) and

(b). However, the significant variability in strength precludes applying this method for drawing strong conclusions on the impact to wetland belowground biomass due to varying hydrologic and ecological processes. The scatter is likely attributed to departures from standard equipment and procedures, heterogeneous soils, pre-consolidation pressure, and plasticity index. Most wetland soils are normally consolidated but extended periods of desiccation at the surface can lead to over-consolidation and higher strengths (e.g., Old Oyster Bayou in [Day et al., 2011](#)). If the soil contains layers or even thin laminations of sand or dense silt, the torque may be much greater than that required if the layers were not present. In coastal marshes that contain roots and shell fragments, the vane shear strength can be artificially increased and inconsistent. Moreover, the fibers and roots in the underlying organic soils may act as localized reinforcement that catches the vane blade and hence lead to strengths that are too high and scattered. This is perhaps the reason for higher soil strength in [Fig. 14\(b\)](#). When these conditions prevail, the results of vane tests may be misleading and not sufficient to form strong conclusions. Moreover, shear measurements are influenced by strain rate and soil anisotropy, i.e., strength is higher in the vertical plane compared to the horizontal plane because of sedimentation and hence existence of laminations. For the vane, 85% of the shearing occurs along the vertical plane while 15% is contributed by the horizontal shearing at the top and bottom of the vane (see [Fig. 6](#)). This creates complexity if the vane test is compared with other shear strength measurements without conducting a study to calibrate the methods to each other. The strain rate is controlled by the rotation rate and the diameter of the vane. Lower strain rates allow more time for the soil to slide, deform, and creep, resulting in lower values of peak strength. In contrast, more rapid strain rates result in a higher apparent strength. Thus, vane measurements are dependent on the operator. It is critical to ensure the strain rate and delay of start between insertion and shearing remain consistent because an order of magnitude difference can yield a 20 percent difference in shear strength ([Cadling and Odenstad, 1950](#)) and the time delay longer than 3 min can yield a higher shear strength ([Flaate, 1965](#)). An additional consideration is the effect of friction between the instrument rod and soil, which adds to the apparent strength of the soil. In the papers discussed, [Turner \(2011\)](#) was the only paper that discussed the rod friction, indicating it was negligible. A correction factor based on plasticity index to reduce the vane strength is proposed by [Terzaghi et al. \(1996\)](#), but this may not be needed in wetland soils because these studies are comparative to evaluate hypotheses. Nevertheless, further study is needed that investigates the effect of rod friction, shearing rate, manufacturer, equipment calibration, and vane dimensions (see ASTM [D2357](#) and [D4648](#)) to quantify the CV of this test method and to help determine if the hand-held vane is sufficiently reproducible in varying wetland soils.

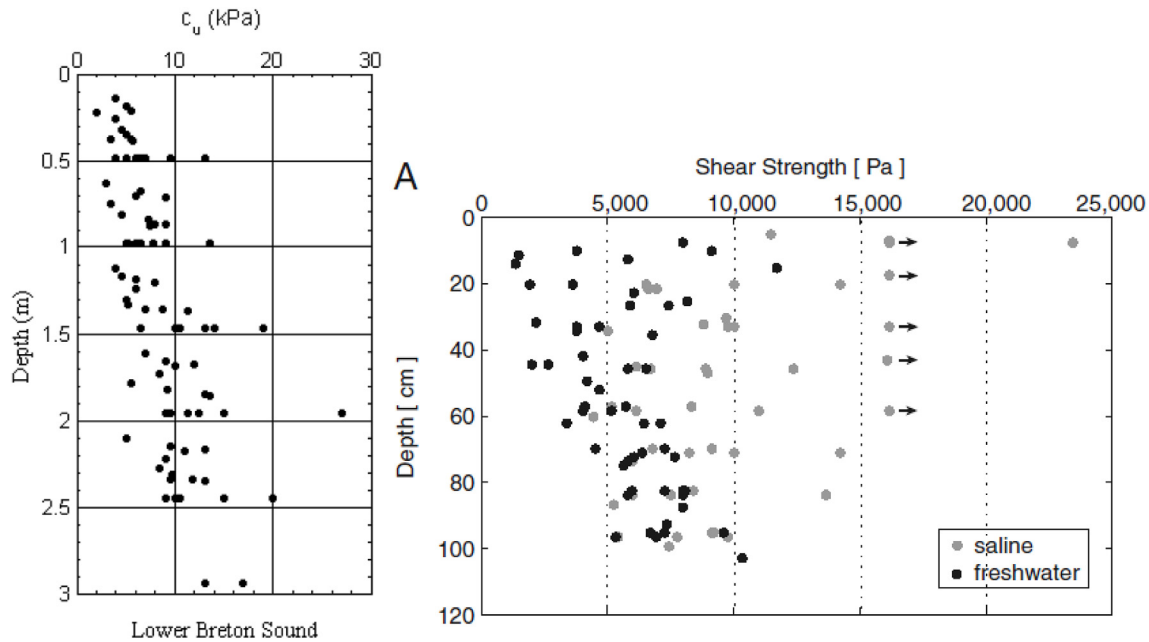


Fig. 14. Examples of shear strength profiles obtained by the hand-held vane test from (a) Lower Breton Sound, Louisiana (Bentley et al., 2015); (b) Breton Sound (Howes et al., 2010).

5.2. Torvane

The torvane or pocket shear vane was originally designed by Slope Indicator Company as a soil testing instrument for the rapid determination of shear strength of cohesive soils in the field or laboratory. Use of torvanes is less common when compared to field vanes due to the smaller range and less precise readings (Blum, 1997). For example, the torvane is applicable for stress ranges under 100 kPa (2000 psf). Applications include sides and bottom of test pits, end of Shelby tube samples, or chunk samples from test pits. Thus, it is meant for shallow inspection purposes. The torvane consists of a disc (vane) with blades on the lower surface that is pressed into the soil (Fig. 15). A torque is applied to the disc when the upper knob is rotated with finger pressure. The torque is resisted by shear stresses in the clay or soil across the lower surface and around the circumferential area of the blades. Similar to the pocket penetrometer, the torvane permits a rapid determination of a large number of strength values with different orientation of failure planes (Terzaghi et al., 1996). It does not specifically indicate exact shear strength characteristics but rather identifies strength variations with depth and zones of weakness in the subsoil. The strengths obtained from the torvane tests must be calibrated against a torvane shear strength correlation before they can be compared with other field and laboratory tests because of the depth effect (deeper soils are stronger because of higher effective stresses). The tests give a crude approximation of the undrained shear strength of the soil mass and should be



Fig. 15. Torvane with various diameter blades (photo courtesy of Humboldt).

compared with others such as the hand-held vane test for reasonable estimate of the undrained shear strength. As with the case for the shear vane, torvane readings of shear strength are dependent on the failure or loading (rotation speed).

Table 3 lists the studies that leveraged the torvane to identify impacts of vegetation on shear strength. In particular, Swarzenski et al. (2008) utilized the torvane to assess the degree of soil decomposition through shear strength measurements in order to study the impacts of river inputs on coastal marsh sustainability in Louisiana. Cores were driven down to 25 cm below ground surface and spilt open in half to allow for torvane readings to be conducted at 5 cm increments. They found that marshes receiving long-term influx of river water (Penchant basin) experienced a more reduced soil substrate and decomposed organic matter consisting of smaller more easily fractionated particles when compared to marshes without river influx (Barataria basin). The average torvane measured shear strength values from 20 readings for the river influenced area and control site were 88.3 ± 8.8 kPa and 206 ± 7.8 kPa, respectively. Plots comparing shear strength with depth or information on the statistical analyses conducted on the readings were not provided within the publication.

McGinnis (1997) linked marsh shear strength measured by a torvane to monitor shoreline movements. In particular, the non-vegetated strengths refer to torvane tests from cores in between vegetation stumps, *Spartina patens* hummocks, while the vegetation strengths were cores taken at a stump. The cores were cut length wise and opened, where upon the torvane tests were performed horizontally in order to study the erosive from a nearby pond rather than from the soil surface. In total, 11 and 4 vegetated and non-vegetated plots were used

Table 3
Summary of torvane studies measuring wetland strength.

Reference	Technique	Location
Chen et al. (2012)	Torvane	Beaulieu Estuary, Southern U.K.
McGinnis (1997)	Trodden Soiltest	Marsh Island, USA, LA
McKee and McGinnis (2003)	Humboldt H-4212	Honduras and Guatemala
Swarzenski et al. (2008)	Humboldt H-4212	Barataria and Penchant Basins, LA

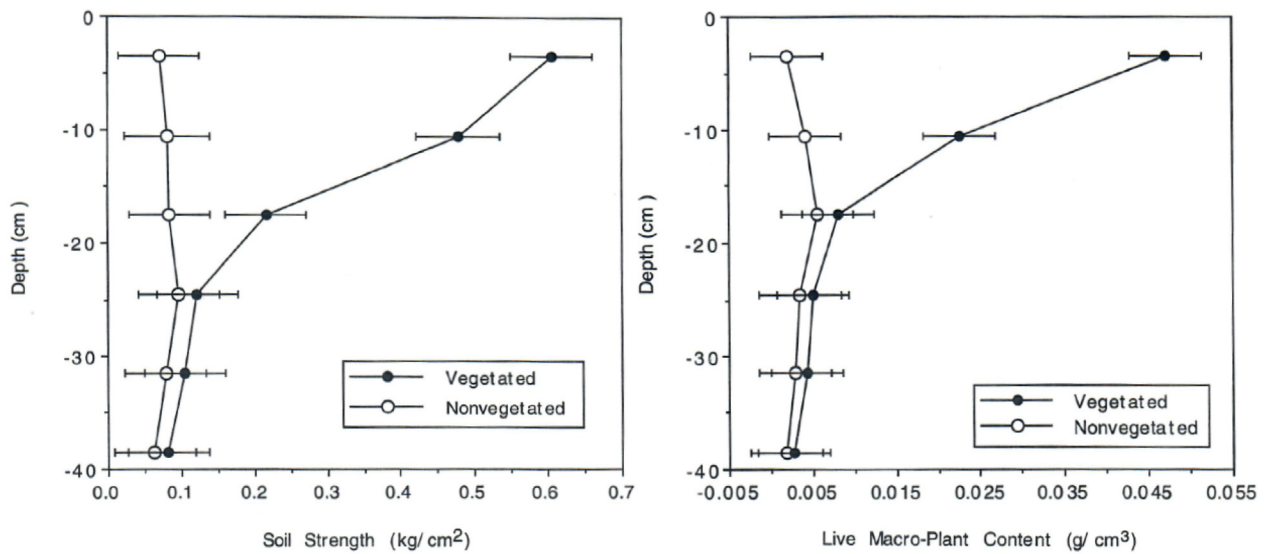


Fig. 16. Soil strength and live plant content profiles with depth in Marsh Island, Louisiana (unit conversion $10.2 \text{ g/cm}^2 = 0.0102 \text{ kg/cm}^2 = 1 \text{ kPa}$). For both plots, the least square means and standard errors are used (from McGinnis, 1997).

for shear strength and live plant content, respectively (i.e., 22 total plots for shear strength and 8 total for plant content). In Fig. 16, the non-vegetated soils yield a constant shear strength of $\sim 0.05 \text{ kg/cm}^2$ ($\sim 5 \text{ kPa}$) with depth, while the vegetated soils exhibited a maximum strength of $\sim 0.6 \text{ kg/cm}^2$ ($\sim 58.8 \text{ kPa}$) near the surface and linearly decreased to the non-vegetated soil strengths at a depth of 25 cm. It was noted that the vegetated surface was on average 7 cm higher than the non-vegetated surface, which created an offset relative to core depth. The vegetated strength profile is very similar to the live micro plant content profile with depth from Graham and Mendelssohn (2014), which indicates the roots are the main contributor to the strength.

McKee and McGinnis (2003) also used a torvane to monitor soil deposition impact on mangrove soil characteristics and root contributions to soil stability. Cores were driven down to 30 cm below the ground surface and readings were conducted at 5 cm increments. Shear strengths at the surface ranged from 0 to $\sim 0.5 \text{ kg/cm}^2$ (0–54 kPa), where both root production and soil deposition positively contributed to soil strengths in mangrove forests. Torvane values were in the typical range of 5 kPa–60 kPa. This is much higher than the hand-held vane shear strengths, which suggests that a calibration needs to occur for a side-by-side comparison. In summary, the torvane allows for a greater number of tests but at the cost of resolution of shear strength measurements (Ding and Loehr, 2019).

5.3. Cone penetrometer

The cone penetration or cone penetrometer test (CPT) provides a higher resolution of resistances with depth when compared to the hand-held vane or torvane, which is useful for evaluation of site stratigraphy, homogeneity and depth to firm layers, voids or cavities, and other discontinuities. The advantage of the CPT is fast and continuous profiling along with repeatable and reliable data. The use of a friction sleeve and pore-water pressure element can provide an estimate of soil classification, and correlations with engineering properties of soils. When properly performed at suitable sites, the test provides a rapid means for determining subsurface conditions. The standard test methodology is summarized in ASTM D5778 (2012), including setting a baseline zero reading before starting a sounding, selecting dimensions for the cone, sensor type and calibration, and penetration rate of the cone. A penetrometer tip with a conical point of 60° apex angle and a cone base area of 8 cm^2 , 10 cm^2 , or 15 cm^2 is advanced through the soil at a constant rate of 2 cm/s (see Fig. 17(a) for schematic). The force on

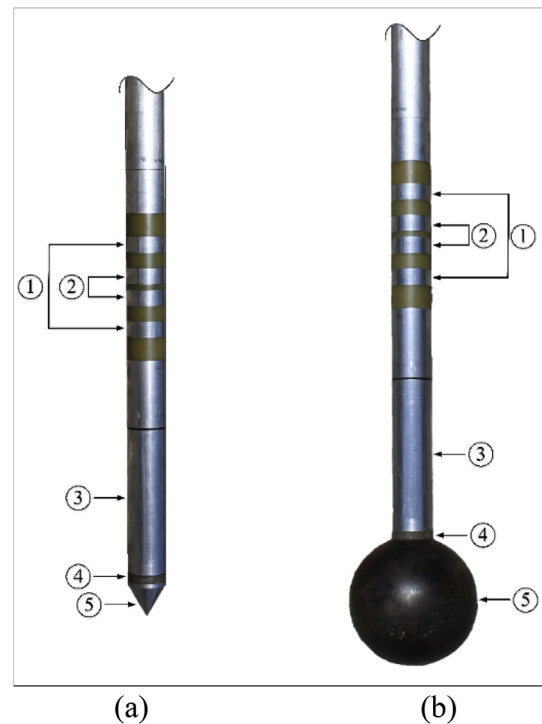


Fig. 17. Schematic of SMRT-CPTu: (a) 8 cm^2 conical tip, and (b) 80 cm^2 ball penetrometers. Stainless steel rings at (1) and (2) represent electrical conductivity and volumetric water content. Arrows (3), (4), and (5) point to sleeve friction, pore-water pressure element, and cone tip, respectively (from Jafari et al. 2019).

the conical point (cone) required to penetrate the soil is measured by a load transducer at 2 cm interval readings as measured by depth potentiometer. The cone tip stress is calculated by dividing the measured force (kN) by the cone base area (8 cm^2) to obtain the cone tip resistance q_c . A friction sleeve is also present on the penetrometer immediately behind the cone tip, and the force exerted on the friction sleeve is measured at similar intervals as the cone tip. The sleeve stress is calculated by dividing the measured axial force by the surface area of the friction sleeve to determine sleeve resistance f_s (Lunne and Robertson, 1997).

Table 4
Summary of cone penetrometer studies in wetlands.

Reference	Technique	Location
Zeeb et al. (1997)	Piezcone penetrometer	Aberjona wetland, Boston, MA, USA
Are et al. (2002)	Mechanical cone penetrometer	Salt marsh in Venice Lagoon and Mississippi Delta
Day et al. (2011)	Mechanical cone penetrometer	Bayou Chitigue and Old Oyster Bayou, LA, USA
Jafari et al. (2019)	Piezcone penetrometer	Terrebonne Bay, LA, USA

Cone penetrometers are also capable of registering pore-water pressure induced during advancement of the penetrometer tip using an electronic pressure transducer (termed piezocones). The dissipation of either positive or negative excess pore-water pressure can be monitored by stopping penetration, holding the depth of penetration constant, and recording pore-water pressure as a function of time. When pore-water pressure becomes constant, it is measuring the equilibrium value (designated u_0) or groundwater surface.

Driving a penetrometer into the ground involves a thrust mechanism and reaction frame. For example, pushing equipment for land applications generally consist of specially built units that are either truck or track mounted. In coastal swamp and wetlands, cone penetrometers are mounted on track-mounted marsh buggies or boats to facilitate subsurface investigations for flood protection and restoration projects. The considerable equipment and mobility of heavy machinery needed to operate CPTs in geotechnical applications has limited their applications in measuring the shear strength of more fragile, shallow wetland soils. Thus, much lighter and more portable driving machinery is required for use on the wetland surface. Table 4 lists several studies that leverage CPTs for understanding wetland strength and stratigraphy. For example, Zeeb et al. (1997) designed a portable piezocone driver to map small-scale heterogeneities in wetland soil types in order to identify groundwater discharge or recharge zones. This was important because it can facilitate transport modeling of solutes, e.g., the hydrogeochemical investigation of the Aberjona River Watershed where a long and well-documented industrial history resulted in contaminated release. The piezocone penetrometer soundings in Zeeb et al. (1997) extended to a depth of 7 m and capable of identifying 50–100 mm thick interbedded soil layers. However, they also found that the tip resistance record lacked detail in the softer soils, indicating the need for greater measurement resolution in the weaker peat layers. Zeeb et al. (1997) recommended a more sensitive load cell, providing resolution of 1% or better of the full-scale value. Improved accuracy in very soft soils can also be accomplished using a T-bar and ball penetrometers (both are 100 cm² or 10 times the typical 10 cm² cone penetrometer; Fig. 17(b) shows an example of a 80 cm² ball penetrometer) because a larger volume of soil is engaged during penetration (Randolph, 2004; Einav and Randolph, 2005; Yafate et al., 2009).

A portable, electrically-driven mechanical cone penetrometer was used by Are et al. (2002) and Day et al. (2012). In particular, Are et al. (2002) describe the instrumentation components and workflow of the thrust system and data collection of the mechanical cone penetrometer system (e.g., Fig. 18(a) shows the general layout and anchor system, adapted from Are et al. (2002). Reproduced with permission from the Coastal Education and Research Foundation, Inc.). The mechanical (also referred to as the Dutch) cone penetrometer can give comparable data to the electric piezocone penetrometer, but there are differences because of the geometry of the cones and friction sleeve sections (ASTM D3441). For example, the mechanical cone takes q_c and f_s measurements at 20 cm and uses inner and outer rods to convey loads uphole. Day et al. (2011) conducted a study on accretionary dynamics and wetland loss in salt marshes surrounding two small ponds at Old Oyster Bayou and Bayou Chitigue in the Mississippi delta near the Atchafalaya River (Fig. 18(a)). In particular, they leveraged the mechanical cone to better explain why the Bayou Chitigue salt marsh is disappearing and Old Oyster Bayou is a stable wetland. For example, Fig. 18(b) shows the

cone resistance and moisture content with depth for both salt marshes. The Old Oyster Bayou exhibits a significantly high resistance (~ 1400 g/cm²) in the first 5 cm, similar to reported higher shear strengths in the desiccated crust found in unsaturated surficial layers (Terzaghi et al., 1996). The higher surface resistance within the top 5 cm is corroborated by a dry bulk density of 0.38 g/cm³, whereas the average dry bulk density from a depth of 5 cm–25 cm is 0.24 g/cm³. In contrast, Bayou Chitigue consists of high moisture contents ($\sim 400\%$) and cone resistance less than 350 g/cm² near the surface. Beyond the rooted depth of 35 cm, the shear resistance of Old Oyster Bayou and Bayou Chitigue are between 200 and 400 g/cm² and generally increase with depth. Day et al. (2011) explain the difference in surface strength by showing that Bayou Chitigue is inundated for a longer duration (85% of the study period) compared to the 15% at Old Oyster Bayou. As a result, anaerobic decomposition via sulfate reduction was present at Bayou Chitigue ($E_h = -120$ mv, $H_2S = 37\text{--}82$ mg/l), where the elevated H_2S caused stress and growth reduction in the *Spartina alterniflora* compared to Old Oyster Bayou ($E_h = -85$ mv, $H_2S = 12$ mg/l). The tip resistance in Fig. 18 is reported in g/cm² so a peak resistance of ~ 1450 g/cm² at Old Oyster Bayou corresponds to 142 kPa. The minimum resistances from 200 to 400 g/cm² beyond the root mat corresponds to $\sim 20\text{--}40$ kPa. The peak and minimum values correspond to measurements made by an electric piezocone penetrometer in Jafari et al. (2019).

Jafari et al. (2019) used an 8 cm² electric piezocone SMRT-CPTu (Soil Moisture, Resistivity, and Temperature; SMRT) that was manually pushed into the subsurface to understand the vertical and spatial variation in geotechnical properties in a salt marsh near Cocodrie, LA. Compared to the mechanical cone, this piezocone (CPTu) also measures pore-water pressure along with soil moisture, resistivity, and temperature (SMRT). Fig. 19 shows the combined geotechnical and ecological parameters obtained from the SMRT-CPTu for two soundings to demonstrate repeatability. The tip resistance was obtained from the ball point tip (projected area of 80 cm²) because the tip resistance resolution was insufficient at a projected area of 8 cm². Because the ball point displaces the soil such that a cavity forms as the piezocone is pushed into the ground, another test with the conical tip was performed to measure the sleeve friction, pore pressure response, volumetric moisture content, and soil electrical conductivity. The sleeve friction in Fig. 19(b) does not register positive values except at the surface due to the reinforced roots and at depths of greater than 1.7 m. This same behavior is observed in the tip resistance, where the vegetation root mat causes a peak of 60 kPa and 100 kPa at 0.1 m before decreasing to a minimum of 20 kPa by 0.3 m. A slight linear increase in resistance is evident until a depth of 1.7 m, which indicates penetration into an inorganic clay layer. Similar tip resistance behavior is evident in Day et al. (2011) and Are et al. (2002). The pore-water pressure response is also linear with depth and greater than the hydrostatic line (see the red dashed line in Fig. 19(c) under the u_2 plot)(in the web version). This suggests that the organic clay was generating excess shear induced pore-water pressure during penetration. The pore-water pressure response increased when entering the inorganic interdistributary clay because the shear strength is higher and hydraulic conductivity is lower, thus the pore-water pressure cannot dissipate. The results in Jafari et al. (2019) demonstrate the combination of tip and sleeve resistance along with pore pressure provide detailed information

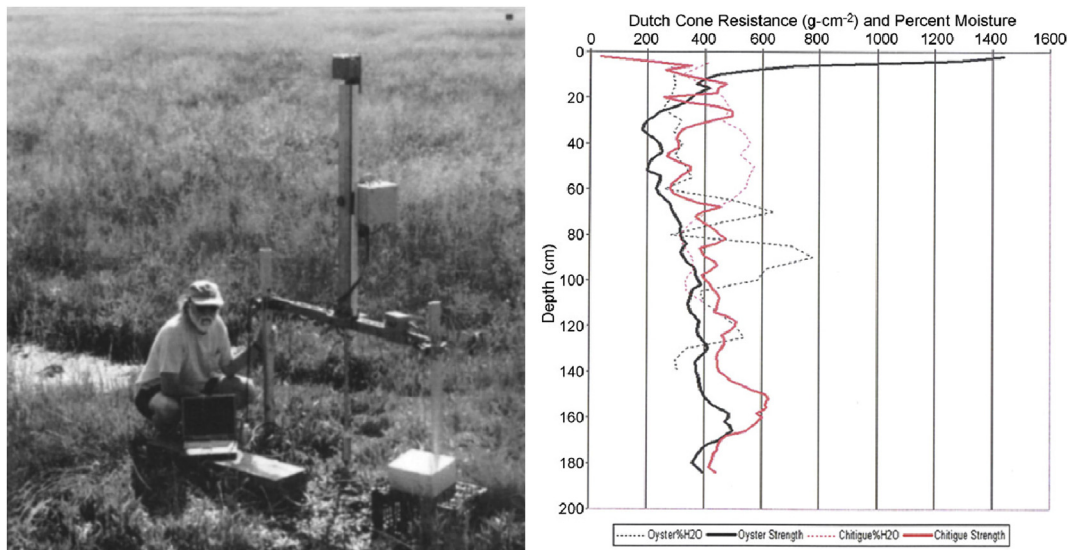


Fig. 18. (a) Photograph of the mechanical cone penetrometer in use in wetlands Venice Lagoon, Italy (Are et al., 2002), and (b) cone penetrometer data from Old Oyster Bayou and Bayou Chitigue, LA (Day et al., 2011).

regarding the thickness of the root mat, shear strength of the organic clay, and lithology of the wetland platform. In addition to these findings, soil moisture and electrical conductivity can be used to determine porosity and bulk density and serve as a proxy for identifying saline soils. However, further research is needed to correlate these measurements to wetland characteristics, e.g., organic, inorganic, and vegetation types from freshwater to salt marshes.

Sufficient data has yet to be measured to determine the uncertainty of cone penetrometer measurements. This is important because it will assist statistical inferences in order to decide if the various shear

strength measurements are statistically different, such as in the range of values in Fig. 19(a). A study was performed by Alshibli et al. (2008) to evaluate the uncertainty in tip resistance (q_c) at the Louisiana Transportation Research Center Accelerated Testing Facility in Port Allen, LA. In particular, they conducted sixteen (16) CPT soundings to a depth of 24.4 m in a dual polar array, where a borehole situated at the center was surrounded by CPTs at radii of 1 m and 2 m. They found the COV with depth for q_c ranged from 7.2% to 36.5%, with an average of 19.6% (Alshibli et al., 2008). It is likely that wetland soils are on the higher end of the COV spectrum reported in Alshibli et al. (2008). As an

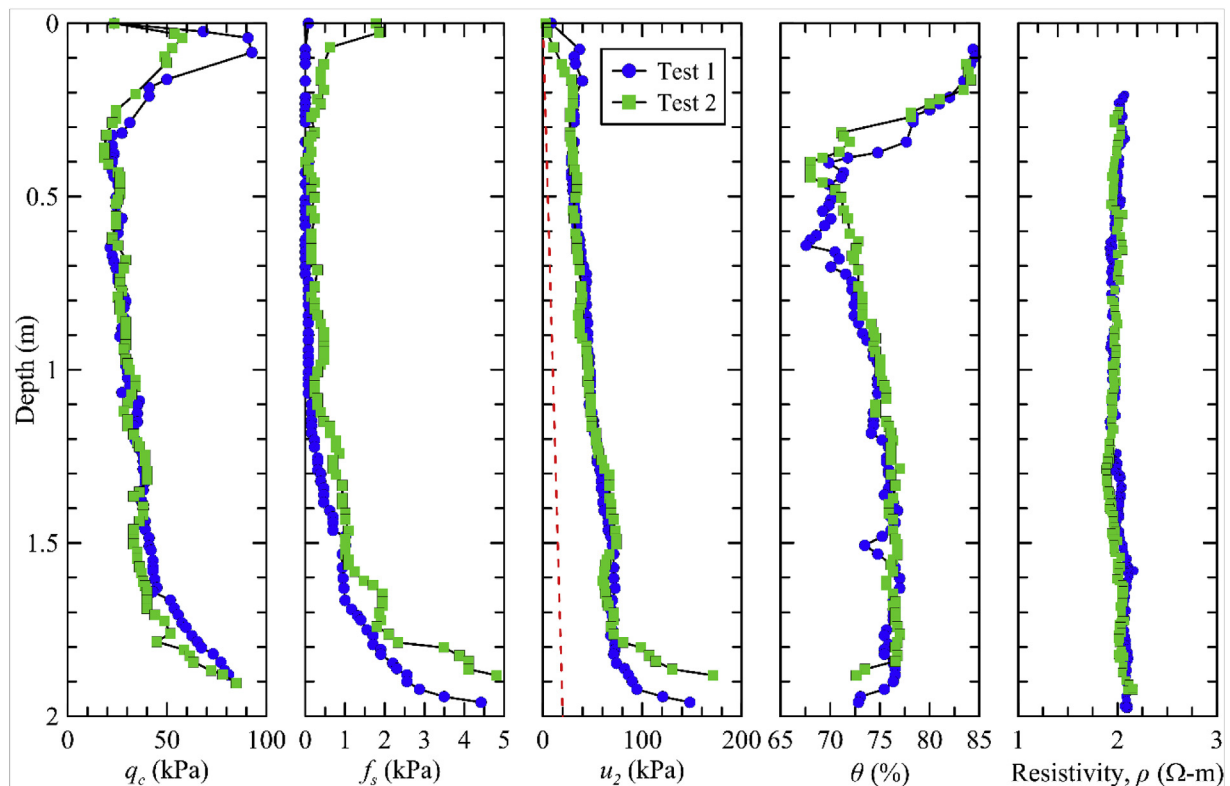


Fig. 19. Suite of geotechnical and ecological parameters obtained from SMRT-CPTu from Jafari et al. (2019) [red dashed line in u_2 plot is the hydrostatic line.]. (For interpretation of the references to color in this figure legend, the reader is referred to the Web version of this article.)



Fig. 20. Diagram and field use of the Wetland Soil Strength Tester (WSST) (modified from Sasser et al., 2018).

example calculation, using a COV of 36.5% and average q_c of 40 kPa in Fig. 19(a), the standard deviation is 14.6 kPa. This demonstrates the imperative need to also explore repeated measurements with piezocones to evaluate the uncertainty.

5.4. wetland soil strength tester

Sasser et al. (2013) developed the Wetland Soil Strength Tester (WSST) to measure wetland surface resistance through the active root zone (~15 cm). The circular, stainless steel metal device has 4 beveled rectangular pins (6.35 mm by 12.7 mm) each 15 cm in length that are inserted into the marsh soil (Fig. 20). The device is then rotated by applying steady pressure with a torque wrench until shear failure is reached in the marsh soil. Sasser et al. (2013, 2018) designed the WSST to determine if marsh soil shear resistance measurements are associated with plant biomass variables and if soil strength varies among different vegetation types. They sampled 52 sites within Louisiana's Coastwide Reference Monitoring System (CRMS) Wetlands program, sampling 11 marsh types and a total of 227 WSST measurements. In general, Sasser et al. (2013, 2018) conducted 3 to 5 replicates at each CRMS site and in some cases up to 10 or 20. Each 0.1 m² plot was processed by first clipping aboveground vegetation to the soil surface. The WSST measured resistance as the peak force applied to the torque wrench required to produce shear failure within the marsh soil matrix. The shear resistances were torque measurements reported in Newton-meters (N-m). Sasser et al. (2013, 2018) refer to the WSST measurements as shear strengths, but the units are in fact a torque (N-m) instead of a stress (kPa). To convert the torque into a shear strength, the torque value needs to account for the shearing surface, similar to the field vane in Eq. (3). Moreover, the WSST only tests the first 15 cm, which precludes the ability to understand shear resistance dynamics with depth and neglects any vegetation root mat contribution to wetland health beyond 15 cm. After the WSST was performed, the belowground biomass was subsequently harvested by extracting a 10 cm diameter core to a depth of 15 cm, which generally corresponds to the zone of most active belowground vegetation production (Sasser et al., 2013, 2018). The CRMS sites with same vegetation type (12 total) were compiled to formulate belowground biomass and shear resistance relationships. For example, seven (7) CRMS sites fall under the dominant vegetation type of Fresh Maidencane (FM), with a total of 46 WSST measurements. The dominant species in the Fresh Maidencane vegetation type was *Panicum hemitomon*, where the total belowground biomass ranged from 2336 g/m² to 4961 g/m². The live portion of the belowground component ranged from 184 g/m² to 3663 g/m². The WSST resistances in the Fresh Maidencane sites ranged from 22 N-m to 177 N-m. Fig. 21 shows that

the Fresh Maidencane vegetation type data exhibited the strongest relationship ($R^2 = 81\%$) of all of the vegetation types in Sasser et al. (2013). The linear regression values across the 12 dominant vegetation types varied from 0.1 to 0.81, with an overall R^2 value of 0.56 for the entire dataset. Thus, Sasser et al. (2013, 2018) report that living belowground biomass was the most consistent indicator of marsh soil resistance (see Fig. 12(c)). The study by Sasser et al. (2013) is a robust analysis of using the WSST to measure soil resistance because it was conducted for a variety of wetland vegetation types over multiple seasons and it was correlated with belowground biomass (consistent with other referenced studies), which was proven as a proxy for wetland soil resistance.

In May 2015, a preliminary assessment of soil strength was also carried using the WSST at two locations near Port Fourchon, LA (Day and Lane, unpublished). Wetland resistance was measured at *Spartina* sp.-dominated, *Avicennia germinans*-dominated, and barren soils at various distances from streamside to the interior marsh. Fig. 22 shows that WSST torque strength decreased from the stream edge to the interior marsh. The *Spartina* sp. strength was at a maximum value near the edge (~35 N-m) before decreasing to a minimum strength of 5–10 N-m at an interior distance of 60–80 m. The WSST results for *Avicennia germinans* also demonstrate a decreasing trend with distance from the streamside to 80 m inland. Based on Fig. 22, the *Avicennia germinans* (mangroves) exhibit on average higher WSST values than *Spartina* sp., with the barren soils experiencing torque values at lower limit of *Spartina* sp. In Fig. 23, the average and ± 1 SE WSST results are shown for inland distances of 20 m and 100 m for *Avicennia germinans* and *Spartina* sp. The low standard errors suggest that the WSST can provide a precise measure of the vegetation surface strength.

5.5. Co-located soil strength measurements

To better characterize sediment erodibility in the receiving basins of two planned river diversion projects (Barataria and Breton Sound Diversions), CPRA funded a data collection effort of co-located soil strength and sediment property measurements. The field data collection effort included direct measurements of sediment erodibility at six study sites that included a range of vegetated substrates, with different types of measurements at the same sites to allow investigation of the relationships among soil strength measurements and sediment properties (Allison et al., 2016). Soil strength measurements including (1) Sed-flume to quantify critical shear stress for erosion; (2) Wetland Soil Strength Tester for *in-situ* soil strength measurements; (3) hand-held vane testers (Geonor H-60 and Geotechnic Geovane) to measure shear strength; and (4) penetrometer (Eijkelkamp Recording Penetrolgger)

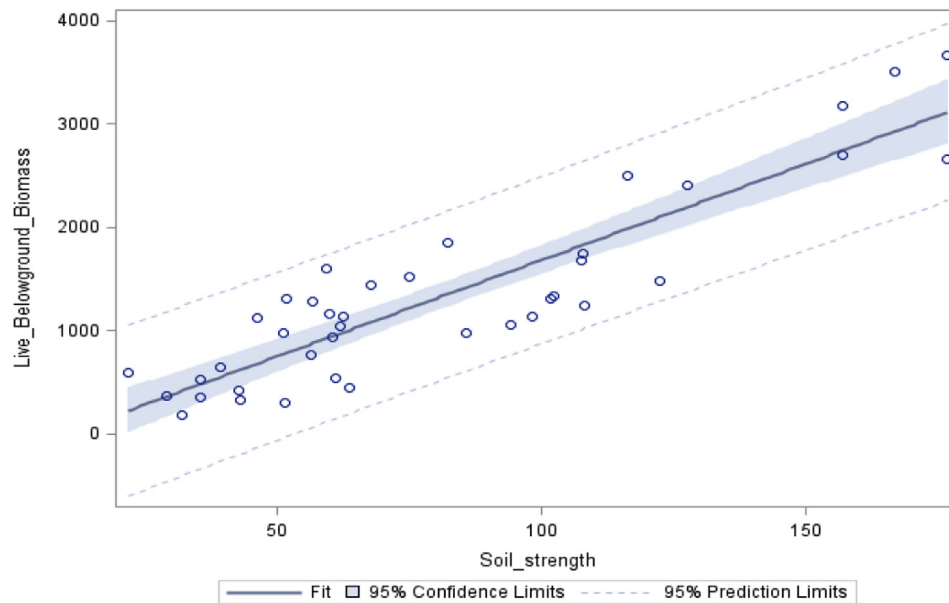


Fig. 21. Regression of live belowground biomass on soil resistance (N-m) for sites sampled in the Fresh Maidencane vegetation type (from Sasser et al., 2013).

measurements of sediment resistance (Allison et al., 2016). Data from the Sedflume measurements show correlative relationships between erosion rates and shear stress, with the erosion rate increasing with increasing shear stress values. The average critical shear stress for erosion varies by site type, with the lowest value (0.17 Pa) at a bare sand site and the highest value (2.26 Pa) at a bare mud site.

A comparison of the data from the two hand-held vane testers (Geonor H-60 and Geotechnic Geovane) for the four sites where data was available for both instruments (bare sand, submerged aquatic vegetation (SAV) sand, SAV mud, and bare mud), shows a strong correlation ($R^2 = 0.94$) of measured vane strength (kPa) values between the two vanes (Fig. 24). The Geovane seems to provide more conservative measurements, however the variability between the two instruments could arise from a variety of factors. The vane strength values ranged from 0.4 to 32 kPa for the Geonor H-60 data, and from 0 to 20.7 kPa for the Geotechnic Geovane. The majority of data points are less than

10 kPa across the four sites, which raises the question if the hand-held vane measurements reflect ecologically significant observations. The WSST data was compared to average shear vane data at vegetated sites only. The shear vane data were averaged down to 15 cm to compare to the WSST data that reaches a maximum of 15 cm. The WSST data ranged from 5.4 to 6.21 N-m of torque across the sampled sites (bare sand, Spartina, SAV sand, SAV mud, and Phragmites). The WSST data more closely correlated to the Geotechnic Geovane data than the A Geonor H-60 data, although the correlations were overall lower than between the two shear vane testers.

Cone penetrometer measurements showed the overall highest forces (up to 750 N) between 40 and 50 cm depth in the bare sand site (Fig. 25). The Phragmites and SAV mud sites show force values below 200 N, whereas the Spartina site indicates higher forces (up to 400 N) below 60 cm depth. Considerable variation in force values were measured at the bare sand site, with the average difference among the six

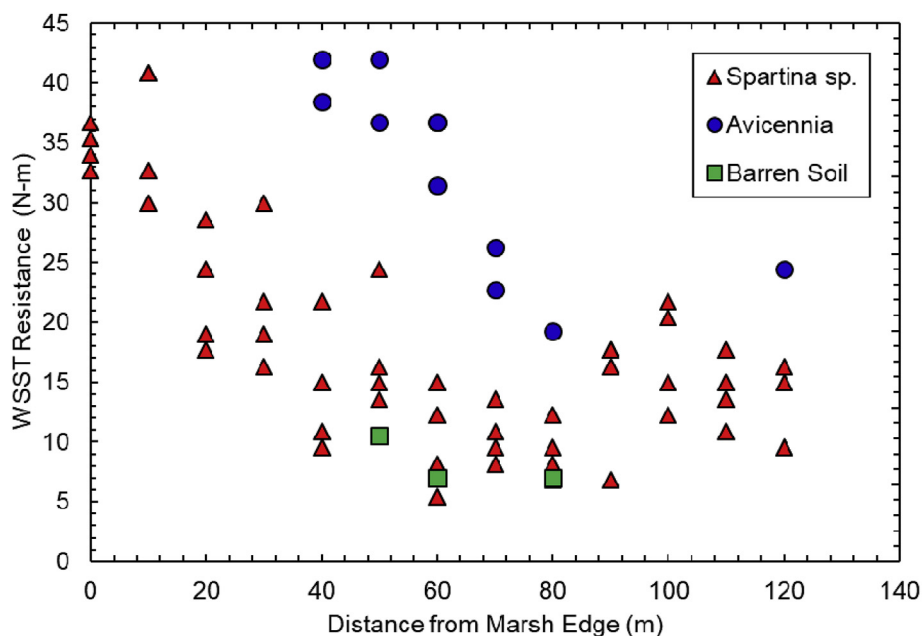


Fig. 22. WSST torque resistance along transects for *Spartina* sp. and *Avicennia germinans*.

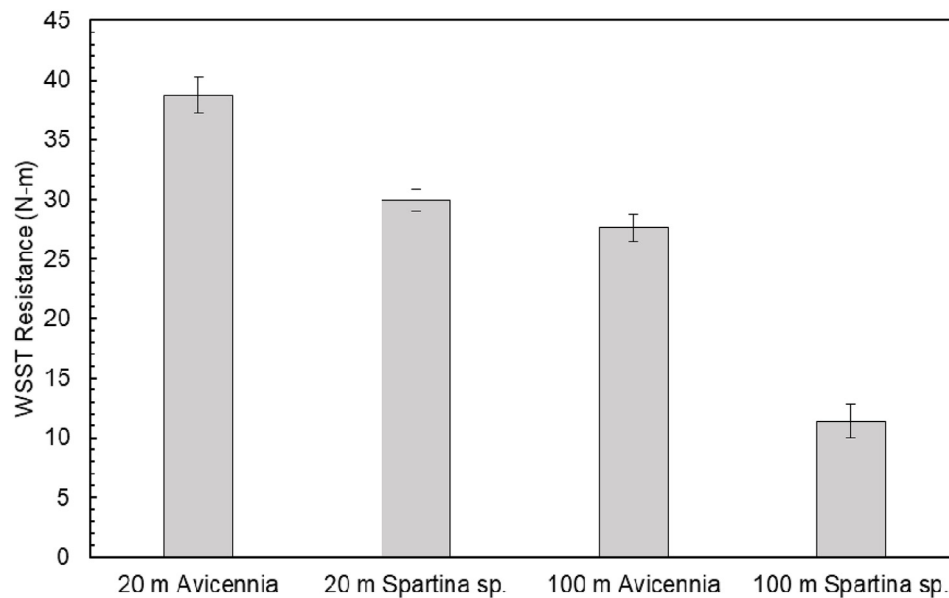


Fig. 23. Comparison of surface wetland strength and WSST standard error for *Spartina* sp. and *Avicennia germinans* at distances inland from the marsh edge.

profiles taken at the same location being 241 N (Fig. 25). A comparison of the mean penetrometer values for the bare sand site and the shear vane data shows a general linear relationship ($R^2 = 0.64$ for Geonor, and $R^2 = 0.65$ for Geotechnic).

6. Instrument performance and statistical inferences

The culmination of this review of shear strength measurements is to provide a discussion that expands on the question concerning what

variation in shear strength or resistance is sufficient to reflect a significant demarcation in geotechnical and ecological behavior of a wetland, from nutrient enrichment, sea level rise, sediment characteristics, oil spills, among other stressors or restoration activities. For example, is a deviation of 5 kPa sufficient to make a justification of an altered shearing resistance or is a larger gap needed (i.e., Figs. 7a, 10 and 12b, 13b, 14)? The cone penetrometer and WSST appear to provide a level of quantification but a grey zone exists that needs to be explored through testing to find what is considered significant. To facilitate

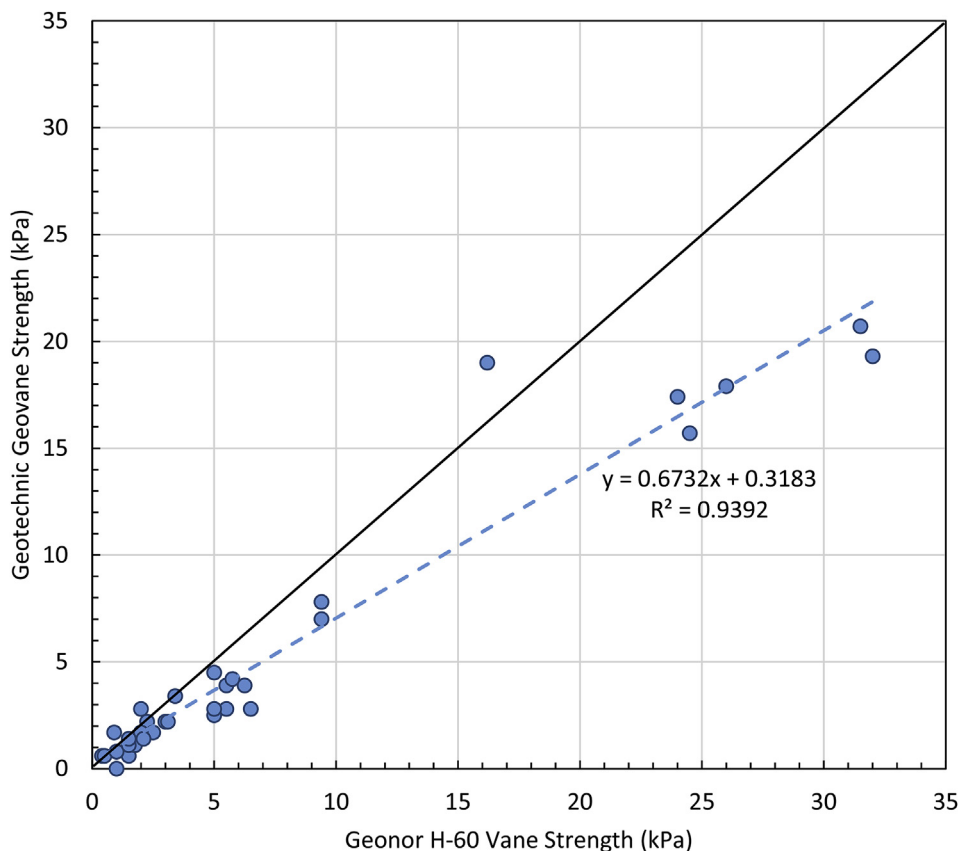


Fig. 24. Comparison of measurements from two shear vane instruments (Geonor Geovane and Geonor H-60). Samples were taken across bare sand, *Spartina*, submerged aquatic vegetation (SAV) sand, submerged aquatic vegetation (SAV) mud, and *Phragmites* sites in coastal Louisiana. Values less than 10 are likely below the level of ecological or geotechnical significance. Solid line is a 1:1 relationship and dashed line is data.

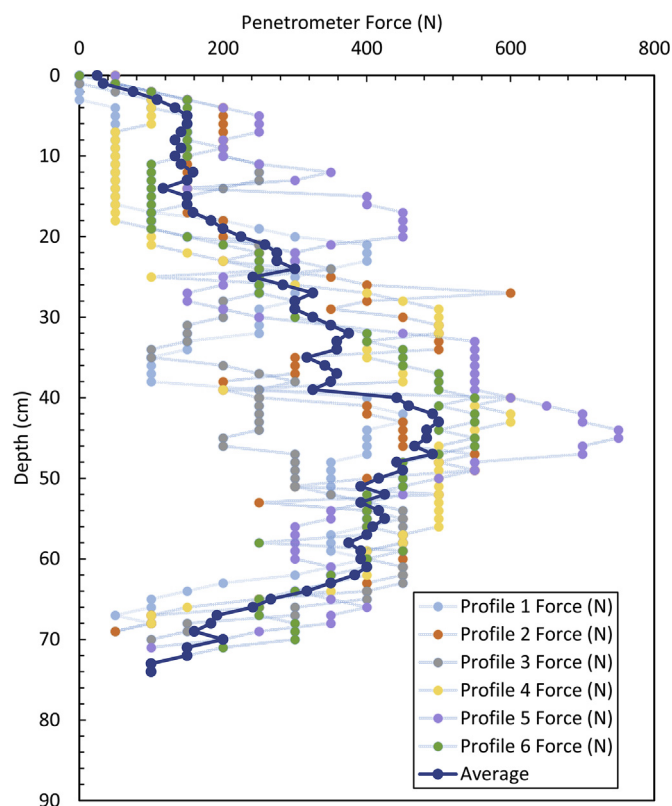


Fig. 25. Comparison of penetrometer measurements at bare sand site in Breton Sound, LA.

discussions, Fig. 26 shows strength measurements made by a Geonor hand-held vane and the piezocone penetrometer described in Jafari et al. (2019). In this case, the sleeve of the piezocone penetrometer was modified to include four 10 cm fins, with the purpose of increasing interactions with the belowground biomass. In November 2019, a field campaign was executed that included conducting five penetrometer and hand-held vane measurements approximately 10 m and 50 m from the marsh edge. Near the interior marsh site, a mudflat was also tested by the penetrometer to quantify sleeve resistance with only soil. Fig. 26(a)–(b) show the raw data for the marsh edge and interior marsh sites, respectively. This data was averaged to create one line in Fig. 26(c) and help facilitate comparisons. In particular, Fig. 26(c) shows that the marsh edge and interior marsh exhibit similar sleeve resistances to a depth of 15 cm, where the marsh edge reaches a peak resistance of 127 kPa at a depth of 25 cm and the interior marsh peaks at 15 cm with a value of 113 kPa. By a depth of 50 cm, the sleeve resistances approach a constant minimum of ~70 kPa and ~30 kPa for the marsh edge and interior marsh, respectively. In comparison, the unvegetated mudflat shows an approximate sleeve resistance of 30 kPa, which matches the interior marsh because of the close proximity of the two sites. Thus, Fig. 26(c) clearly demonstrates that at a depth of 30 cm, a significant difference of 60 kPa in sleeve resistance was observed moving from the marsh edge to the interior marsh. As a qualitative comparison, walking on the marsh edge was effortless. In contrast, trekking towards the interior marsh resulted in sinking to shin depth. Over this 40 m distance, a significant difference in geotechnical and ecological behavior was observed. From an ecological viewpoint, this observation is substantiated because more flooding occurs in the interior marsh, which leads to a more reduced environment, hydrogen sulfide production, and reduced vegetation productivity. The harvested aboveground vegetation also reflects this reduced productivity because the marsh edge was 176 stems/m² while the interior marsh was 125 stems/m². In contrast, the hand-held vane shows higher strengths and

more scatter in the upper 40 cm before approaching a strength less than 10 kPa to a depth of 100 cm. More importantly, the vane device was unable to show the change in strength from marsh edge to the interior as clearly as the cone penetrometer. This review further indicates that hand-held vanes can provide a general profile of strength, but are unable to provide quantitative information on shear strength. The data and corresponding discussion indicate that the cone penetrometer is a reasonable tool to measure spatial and temporal variation in wetland, even the depth of peak belowground biomass in Fig. 26(c), that can relate to anticipated and significant ecological variations. In this case, a sleeve resistance of 40 kPa–60 kPa reflected a major change in vegetation strength. Applying this methodology to different coastal basins, restoration projects, vegetation and soil types, and other environmental stressors will facilitate a better understanding how the hydrology, ecology, and geotechnical behavior of wetlands can change in space and time.

7. Summary and recommendations for future work

This paper presents a review of shear strength measurements in wetlands, which can be used to make inferences of wetland health on the influence of impacts such as nutrients, sediments or flooding. As part of the review, this paper provides an introductory overview of soil mechanics principles for wetland ecologists because of the increasing frequency of geotechnical measurements used to make inferences and conclusions. Understanding effective stress is important because all measurable effects of soil behavior, such as compression, deformation, and strength, are due to changes in effective stress. The review of shear strength describes the difference between drained and undrained strengths and the process geotechnical engineers undergo to ensure field and laboratory undrained shear strength measurements are comparable. The addition of roots or shells in the soil matrix adds significant complexity to the measurement of in-situ shear strength. As a result, the majority of the papers focused on in-situ techniques such as the hand-held vane, torvane, cone penetrometer, and wetland soil strength tester to measure the shear strength or resistance of wetland soils. A larger component of the review is focused on the hand-held vane because of the many prior studies, with only a select more recent studies utilizing the WSST (Sasser et al., 2013, 2018) and cone penetrometer (Are et al., 2002; Day et al., 2011; Jafari et al. 2019). The torvane is not recommended for making wetland strength measurements because it only gives a crude approximation of the undrained shear strength.

In coastal marshes that contain roots and shell fragments, the hand-held vane and torvane strengths were found to be artificially increased and inconsistent. This constitutes a significant drawback of the hand-held vane device. In fact, ASTM D4648 (2016) states that the vane test is not recommended in any soil that permits drainage or dilates during the test period, such as stiff clays, sands or sandy silts, or soils where stones, large roots, or shells are encountered by the vane in such a manner as to influence the results. In addition, insertion of the vane cuts roots in the soil, creating an altered soil structure. Many of the studies using the hand-held vane use statistics to make inferences. These studies show that the hand-held vane method is capable of outlining the general trend in shear strength with depth and across various vegetation communities and environmental conditions. However, the significant variability in strength precludes applying this method for drawing conclusions on the impact to wetland belowground biomass due to varying hydrologic and ecological processes. The scatter is likely attributed to departures from standard equipment and procedures, heterogeneous soils, pre-consolidation pressure, and plasticity index. Showing the individual vane measurements along with $\mu \pm SD$ for each increment and study variable is more beneficial and practical for drawing conclusions. Moreover, 3 to 6 measurements may not be a sufficient number of measurements to form conclusions, especially if the coefficient of variation (COV) for undrained shear strengths

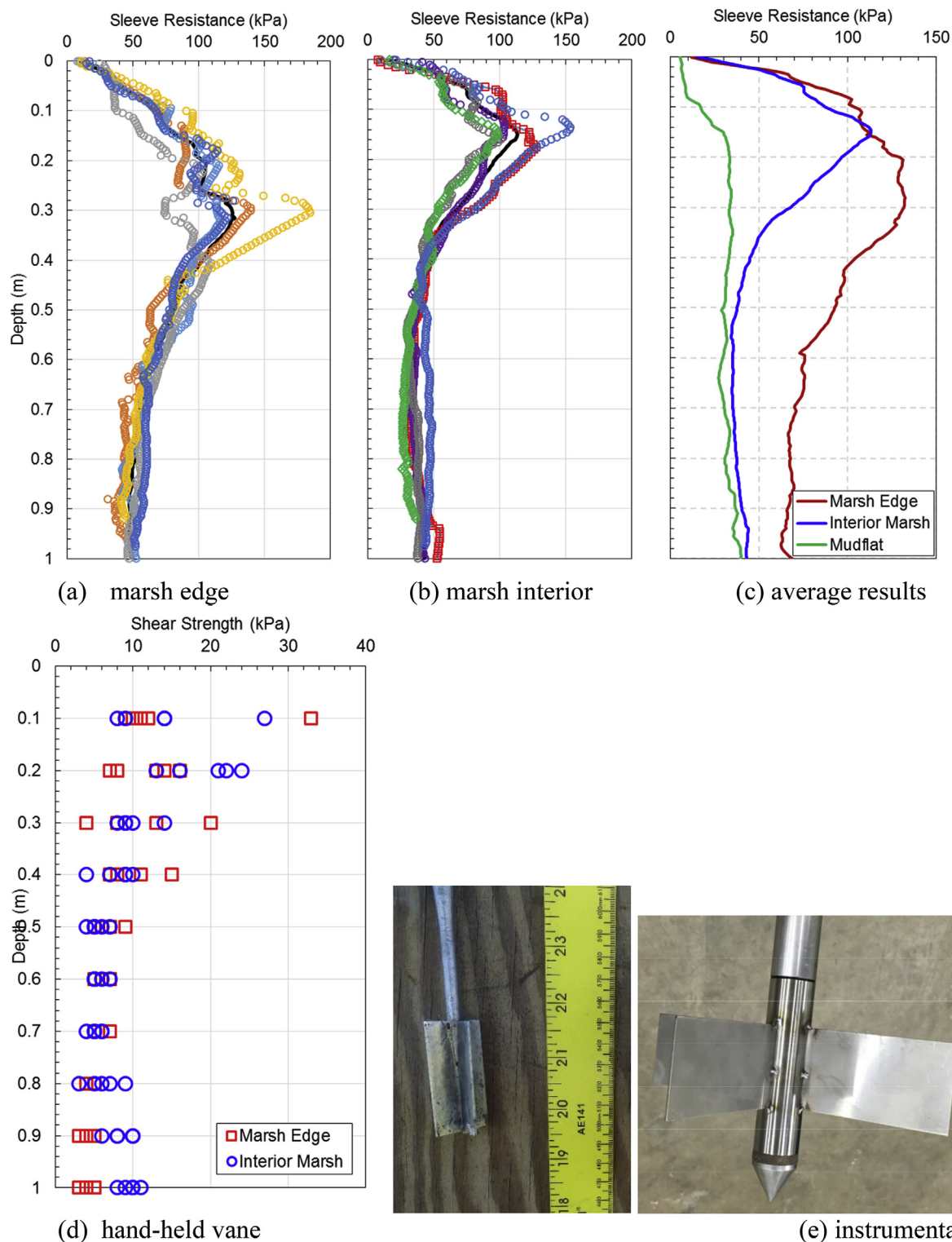


Fig. 26. (a) Marsh edge, (b) marsh interior, and (c) average results of strength measurements from a modified sleeve piezocone penetrometer and (d) shear strength measurements from a hand-held vane in Terrebonne Bay near Cocodrie, LA. (e) A comparison of hand-held vane (left) and modified penetrometer (right).

reported in geotechnical engineering literature ranges from 13% to 40% (Harr, 1984; Kulhawy, 1992; Lacasse and Nadim, 1997; Duncan, 2000). Information about the soil and vegetation properties for the vane shear strength profile is recommended to explain the observed measurements. Moreover, providing the entire data set and corresponding statistics for the shear strength measurements is recommended for the reader to make inferences, and further studies are needed to define the COV of

the hand-held vane for wetland soils. In general, care should be taken in drawing conclusions where differences between tests (i.e., for sediments, nutrients, or flooding) is less than 10 kPa. Viewing changes in other soil index properties (moisture content, organic content, and sediment type and particle size) can also help substantiate differences in wetland strengths.

The results of this review indicate that there is a need to identify and

develop a consistent in-situ methodology to assess marsh shear strength over a full range of vegetation types and environmental conditions. This lack of a uniform assessment methodology creates uncertainty when comparing different investigations on marsh soils and adds complexity for attempting to draw broad conclusions from multiple sites across Louisiana and beyond. For example, a side-by-side comparison of the hand-held vane, WSST, and cone penetrometer is needed in order to directly understand the advantages and limitations of each method and potentially develop a relationship amongst the test methods. This will also help convert the WSST torque measurements into actual shear strengths. Moreover, the uncertainty of shear strength for each in-situ test method is greatly needed in order to establish the number of replicates at a given site and statistical analyses that should be used for making inferences. The aforementioned needs can be accomplished by a comprehensive study that considers and accounts for vegetation type and species, hydrology, sediment accretion, inorganic or organic substrate, nutrient input, salinity, wetland biogeochemistry, and seasonal changes of vegetation production. Sasser et al. (2013, 2018) leveraged the CRMS sites, which contains long-term historical data for the environmental conditions. It is important to collate the in-situ methods and provide sufficient area for adequate replicates to satisfy a robust experimental design. The data collection also requires the corresponding biogeochemical properties, geotechnical index properties (e.g., soil type, bulk density), total belowground production and other appropriate variables sampled by depth (similar to reported by Graham and Mendelsohn, 2014). A standardized and calibrated tool to measure shear strength will assist managers in assessing wetlands impacted by environmental stressors (oil spills, hurricanes, hydrologic alteration, sea level rise, and subsidence) and in tracking success of restoration and climate adaptation actions.

Acknowledgments

aSupport was provided by the Louisiana Coastal Protection and Restoration Authority Interagency Agreement No. 4400008905 – Task Order 2. Support for this research was provided by the Louisiana Coastal Protection and Restoration Authority (CPRA) and administered by Louisiana Sea Grant (LSG) through its Coastal Science Assistantship Program (CSAP).

This report is contribution number ORD- 030078 of the U.S. EPA's Office of Research and Development, National Health and Environmental Effects Research Laboratory, Atlantic Ecology Division. The views expressed in this article are those of the authors and do not necessarily represent the views or policies of the U.S. Environmental Protection Agency. Mention of trade names or commercial products does not constitute endorsement or recommendation for use.

Appendix A. Supplementary data

Supplementary data to this article can be found online at <https://doi.org/10.1016/j.ecss.2019.106394>.

References

- Allison, M.A., Carruthers, T.J.B., Ramachandiran, C., Baustian, M.M., Meselhe, E.A., Pratt, T., Smith, J., Taylor, M., Priestas, A., Kirkland, T., 2016. TO15/16: Sediment Erodibility in Outfall Areas of Barataria and Breton Sound Geotechnical Field Investigation. The Water Institute of the Gulf, Baton Rouge, LA.
- Alshibli, K.A., Okeil, A., Alramahi, B., 2008. Update of Correlations between Cone Penetration and Boring Log Data. Louisiana Transportation Research Center, pp. 147–157.
- Ameen, A.D., Koller, A.S., Taylor, C.M., 2017. Vegetation and shear strength in a delta-splay mouth bar. *Wetlands* 37 (6), 1159–1168. <https://doi.org/10.1007/s13157-017-0948-7>.
- Anisfeld, S.C., Hill, T.D., 2012. Fertilization effects on elevation change and belowground carbon balance in a Long Island Sound tidal marsh. *Estuar. Coasts* 35, 201–211.
- Are, D., Kemp, G.P., Giustina, F., Day, J., Scarton, F., 2002. A portable, electrically-driven Dutch cone penetrometer for geotechnical measurements in soft estuarine sediments. *J. Coast. Res.* 18, 372–378.

- ASTM D2573/D2573M-15, 2015. Standard Test Method for Field Vane Shear Test in Saturated Fine-Grained Soils. ASTM International, West Conshohocken, PA.
- ASTM D3441-16, 2016. Standard Test Method for Mechanical Cone Penetration Testing of Soils. ASTM International, West Conshohocken, PA.
- ASTM D4648/D4648M-16, 2016. Standard Test Methods for Laboratory Miniature Vane Shear Test for Saturated Fine-Grained Clayey Soil. ASTM International, West Conshohocken, PA.
- ASTM D5778-12, 2012. Standard Test Method for Electronic Friction Cone and Piezocone Penetration Testing of Soils. ASTM International, West Conshohocken, PA.
- Barras, J., Brock, J., Morton, R.A., Travers, L.J., 2010. Remotely Sensed Imagery Revealing the Effects of Hurricanes Gustav and Ike on Coastal Louisiana. vol. 2008.
- Bendoni, M., Francalanci, S., Cappietti, L., Solari, L., 2014. On salt marshes retreat: experiments and modeling toppling failures induced by wind waves. *J. Geophys. Res.* Earth Surface 119 (3), 603–620. <https://doi.org/10.1002/2013JF002967>.
- Bendoni, M., Mel, R., Solari, L., Lanzoni, S., Francalanci, S., Oumeraci, H., 2016. Insights into lateral marsh retreat mechanism through localized field measurements. *Water Resour. Res.* 52 (2), 1446–1464. <https://doi.org/10.1002/2015WR017966>.
- Bentley, S., Xu, K., Chen, Q., 2015. Data Report Submitted to the Water Institute of the Gulf Task Order 16: Geological and Geotechnical Characterization of the Lower Breton Sound Diversion Receiving Basin. vol. 2015. Coastal Studies Institute, pp. 1–66.
- Bertness, M.D., 1991. Zonation of *Spartina patens* and *Spartina alterniflora* in new England salt marsh. *Ecology* 72 (1), 138–148.
- Bertness, M.D., Miller, T., 1984. The distribution and dynamics of *Uca pugnax* (Smith) burrows in a new England salt marsh. *J. Exp. Mar. Biol. Ecol.* 83 (3), 211–237.
- Blum, P., 1997. Physical properties handbook: a guide to the shipboard measurement of physical properties of deep-sea cores. College Station, Texas, USA. <http://www-odp.tamu.edu>.
- Blum, M.D., Roberts, H.H., 2012. The Mississippi delta region: past, present, and future. *Annu. Rev. Earth Planet Sci.* 40 (1), 655–683.
- Briaud, J.L., 1992. The Pressuremeter. Taylor and Francis, London, pp. 422.
- Cadling, L., Odensad, S., 1950. The vane borer. In: *Proc. Swedish Geot. Inst.* vol. 2. pp. 88.
- Carlson, L., 1948. Determination in situ of the shear strength of undisturbed clay. In: *Proc. 2nd Int. Conf. S.M.* I. pp. 265.
- Chen, Y., Thompson, C.E.L., Collins, M.B., 2012. Saltmarsh creek bank stability: biostabilization and consolidation with depth. *Cont. Shelf Res.* 35, 64–74. <https://doi.org/10.1016/j.csr.2011.12.009>.
- Chen, Q., Ozeren, Y., Zhang, G., Wren, D., Wu, W., Jadhav, R., Parker, K., Pant, H., 2013. Laboratory and field investigations of marsh edge erosion. In: Abdul, K., Wu, W. (Eds.), *Sediment Transport: Monitoring, Modeling and Management*. vol. 2013. Nova Science Publishers, Inc, pp. 311–337 390 pp.
- Cofie, P., 2001. Mechanical Properties of Tree Roots for Soil Reinforcement Models. (S.n., S.I.).
- Cola, S., Sanavia, L., Simonini, P., Schrefler, B.A., 2008. Coupled thermohydrromechanical analysis of Venice lagoon salt marshes. *Water Resour. Res.* 44 (5).
- Coleman, J.M., Gagliano, S.M., 1960. Sedimentary Structures: Mississippi River Deltaic Plain, vol. 12 Society of Economic Paleontologists and Mineralogists AAPG Special Publication.
- Collins, A.L., Anthony, S.G., 2008. Assessing the likelihood of catchments across England and Wales meeting 'good ecological status' due to sediment contributions from agricultural sources. *Environ. Sci. Policy* 11 (2), 163–170.
- Collison, A.J.C., Anderson, M.G., Lloyd, D.M., 1995. Impact of vegetation on slope stability in a humid tropical environment – a modelling approach. *Proc. Inst. Civ. Eng. Wat., Marit. Energy* 112 (2), 168–175.
- Coops, H., Geilen, N., Verheij, H.J., Boeters, R., van der Velde, G., 1996. Interactions between waves, bank erosion and emergent vegetation: an experimental study in a wave tank. *Aquat. Bot.* 53 (3), 187–198.
- Couvillion, B.R., Beck, H., Schoolmaster, D., Fischer, M., 2017. Land area change in coastal Louisiana (1932 to 2016). U.S. Geological Survey Sci. Investig. Map 3381, 16 (pamphlet).
- Coastal Protection, Restoration Authority, 2017. Louisiana's Comprehensive Master Plan for a Sustainable Coast.
- Darby, F.A., Turner, R.E., 2008a. Below- and aboveground biomass of *Spartina alterniflora*: response to nutrient addition in a Louisiana salt marsh. *Estuar. Coasts* 31, 326–334.
- Darby, F.A., Turner, R.E., 2008b. Effects of eutrophication on salt marsh root and rhizome accumulation. *Mar. Ecol. Prog. Ser.* 363, 63–70.
- Darby, F.A., Turner, R.E., 2008c. Below- and aboveground *Spartina alterniflora* production in a Louisiana salt marsh. *Estuar. Coasts* 31, 223–231.
- Day, J.W., Scarton, F., Rismondo, A., Daniele, A., 1998. Rapid deterioration of a salt marsh in Venice lagoon, Italy. *J. Coast. Res.* 14 (2), 583–590.
- Day Jr., J.W., Gunn, J.D., Folan, W.J., Yáñez-Arancibia, A., Horton, B.P., 2007. Emergence of complex societies after sea level stabilized. *Eos, Trans. Am. Geophys. Union* 88 (15), 169–170.
- Day, J.W., Alejandro, Y.-A., William, J.M., 2009. Management approaches to address water quality and habitat loss problems in coastal ecosystems and their watersheds: ecotechnology and ecological engineering. *Ocean Yearb. Online* 23 (1), 389–402.
- Day, J.W., Kemp, G.P., Reed, D.J., Cahoon, D.R., Boumans, R.M., Suhayda, J.M., Gambrell, R., 2011. Vegetation death and rapid loss of surface elevation in two contrasting Mississippi delta salt marshes: the role of sedimentation, autocompaction and sea-level rise. *Ecol. Eng.* 37 (2), 229–240.
- Day, J., Hunter, R., Keim, R.F., DeLaune, R., Shaffer, G., Evers, E., Reed, D., Brantley, C., Kemp, P., Day, J., Hunter, M., 2012. Ecological response of forested wetlands with and without large-scale Mississippi River input: implications for management. *Ecol. Eng.* 46, 57–67.

- Day, J., Lane, R., Moerschbaecher, M., DeLaune, R., Mendelssohn, I., Baustian, J., Twilley, R., 2013. Vegetation and soil dynamics of a Louisiana estuary receiving pulsed Mississippi River water following hurricane Katrina. *Estuar. Coasts* 36, 1–18.
- Day, J.W., Agboola, J., Chen, Z., D'Elia, C., Forbes, D.L., Giosan, L., Kemp, P., Kuenzer, C., Lane, R.R., Ramachandran, R., Syvitski, J., Yañez-Arancibia, A., 2016. Approaches to defining deltaic sustainability in the 21st century. *Estuar. Coast Shelf Sci.* 183, 275–291.
- Day, J., Lane, R., D'Elia, C., Wiegman, A., Rutherford, J.S., Shaffer, G., Brantley, C.G., Kemp, G., 2018. Large Infrequently Operated River Diversions for Mississippi Delta Restoration. pp. 113–133.
- Deegan, L.A., Bowen, J.L., Drake, D., Fleeger, J.W., Friedrichs, C.T., Galván, K.A., Hobbie, J.E., Hopkinson, C., Johnson, D.S., Johnson, J.M., LeMay, L.E., Miller, E., Peterson, B.J., Picard, C., Sheldon, S., Sutherland, M., Vallino, J., Warren, R.S., 2007. Susceptibility of Salt Marshes to Nutrient Enrichment and Predator Removal, vol. 17. pp. S42–S63 sp.5.
- Deegan, L.A., Johnson, D.S., Warren, R.S., Peterson, B.J., Fleeger, J.W., Fagherazzi, S., Wollheim, W.M., 2012. Coastal eutrophication as a driver of salt marsh loss. *Nature* 490, 388–392.
- DeJong, J.T., Mortensen, B.M., Martinez, B.C., Nelson, D.C., 2010. Bio-mediated soil improvement. *Ecol. Eng.* 36 (2), 197–210.
- Delaune, R., Pezeshki, S., 1988. Relationship of mineral nutrients to growth of *Spartina alterniflora* in Louisiana salt marshes. *Northeast Gulf Sci.* 10 (1).
- Delaune, R.D., Patrick, W.H., Buresh, R.J., 1978. Sedimentation rates determined by ¹³⁷Cs dating in a rapidly accreting salt marsh. *Nature* 275 (5680), 532–533.
- DeLaune, R.D., Nyman, J.A., Patrick, W.H., 1994. Peat collapse, ponding and wetland loss in a rapidly submerging coastal marsh. *J. Coast. Res.* 10, 1021–1030.
- Ding, D., Loehr, J.E., 2019. Variability and bias in undrained shear strength from different sampling and testing methods. *J. Geotech. Geoenviron. Eng.* 145 (10), 04019082.
- Duncan, J.M., 2000. Factors of Safety and Reliability in Geotechnical Engineering. 126 (4), 307–316.
- Durocher, M.G., 1990. Monitoring spatial variability of forest interception. *Hydrol. Process.* 4 (3), 215–229.
- Einav, I., Randolph, M.F., 2005. Combining Upper Bound and Strain Path Methods for Evaluating Penetration Resistance, vol. 63. pp. 1991–2016 14.
- Fagherazzi, S., Kirwan, M.L., Mudd, S.M., Guntenspergen, G.R., Temmerman, S., D'Alpaos, A., van de Koppel, J., Rycbycz, J.M., Reyes, E., Craft, C., Clough, J., 2012. Numerical Models of Salt Marsh Evolution: Ecological, Geomorphic, and Climatic Factors, vol. 50 1.
- Fennessy, S., Jacobs, A., Kentula, M., 2007. An Evaluation of Rapid Methods for Assessing the Ecological Condition of Wetlands.
- Flaate, K., 1965. Field vane tests with delayed shear. In: Paper Presented at 5th Pacific Area National Meeting of the ASTM (Seattle).
- Fox, L., Valiela, I., Kinney, E.L., 2012. Vegetation cover and elevation in long-term experimental nutrient-enrichment plots in Great Sippewissett Salt Marsh, Cape Cod, Massachusetts: implications for eutrophication and sea level rise. *Estuar. Coasts* 35, 445–458.
- Graham, S.A., Mendelssohn, I.A., 2014. Coastal wetland stability maintained through counterbalancing accretionary responses to chronic nutrient enrichment. *Ecology* 95, 3271–3283.
- Gray, D.H., Sotir, R.B., 1996. *Biotechnical and Soil Bioengineering Slope Stabilization: A Practical Guide for Erosion Control*. Wiley.
- Harr, M.E., 1984. Reliability-based Design in Civil Engineering. vol. 1984 Dept. of Civil Engineering, North Carolina State University, Raleigh, N.C Henry M. Shaw Lecture.
- Herrick, J.E., Jones, T.L., 2002. A dynamic cone penetrometer for measuring soil penetration resistance. *Soil Sci. Soc. Am. J.* 66.
- Holtz, R.D., Kovacs, W.D., Sheahan, T.C., 2011. *Introduction to Geotechnical Engineering*, an, second ed. Pearson.
- Howes, N.C., Fitzgerald, D.M., Hughes, Z.J., Georgiou, I.Y., Kulp, M.A., Miner, M.D., Smith, J.M., Barras, J.A., 2010. Hurricane-induced failure of low salinity wetlands. *Proc. Natl. Acad. Sci.* 107, 14014–14019.
- Jadhav, R.S., Chen, Q., Smith, J.M., 2013. Spectral distribution of wave energy dissipation by salt marsh vegetation. *Coast Eng.* 77, 99–107.
- Jafari, N.H., Stark, T.D., Leopold, A.L., Merry, S.M., 2015. Three-dimensional levee and floodwall underseepage. *Can. Geotech. J.* 53 (1), 72–84.
- Jafari, N.H., Harris, B.D., Cadigan, J.A., Chen, Q., 2019. Piezocone penetrometer measurements in coastal Louisiana wetlands. *Ecol. Eng.* 127, 338–347.
- Johnson, D.S., Warren, R.S., Deegan, L.A., Mozdzer, T.J., 2016. Saltmarsh Plant Responses to Eutrophication, vol. 26. pp. 2649–2661 8.
- Kearney, M., Rogers, S., A., 2010. Forecasting sites of future coastal marsh loss using topographical relationships and logistic regression. *Wetl. Ecol. Manag.* 18, 449–461. <https://doi.org/10.1007/s11273-010-9178-y>.
- Kim, S.B., Baglan, N., Davis, P.A., 2013. Current understanding of organically bound tritium (OBT) in the environment. *J. Environ. Radioact.* 126, 83–91.
- Knutson, P., 1988. Role of Coastal Marshes in Energy Dissipation and Shore Protection. pp. 161.
- Kuecher, Gerald Joseph, 1994. *Geologic Framework and Consolidation Settlement Potential of the Lafourche Delta, Topstratum Valley Fill; Implications for Wetland Loss in Terrebonne and Lafourche Parishes, Louisiana*. LSU Historical Dissertations and Theses. pp. 5734. https://digitalcommons.lsu.edu/gradschool_disstheses/5734175.
- Kulhawy, F.H., 1992. On the evaluation of soil properties. *ASCE Geotech. Spec. Publ.* 31, 95–115.
- Kulhawy, F.H., Mayne, P.W., 1990. *Manual on Estimating Soil Properties for Foundation Design*. Electric Power Research Institute EL-6800. Electric Power Research Institute, Palo Alto, Calif Project 1493-6.
- Lacasse, S., Nadim, F., 1997. Uncertainties in characterizing soil properties. In: In: Shackleford, C.D., Nelson, P.P., Roth, M.J.S. (Eds.), *Uncertainty in the Geologic Environment: from Theory to Practice*, Geotechnical Special Publication, vol. 58. ASCE, New York, pp. 49–75.
- LaRochelle, P., Roy, M., Tavenas, F., 1973. Field measurements of cohesion in champlain clays. In: *Proceedings of the 8th International Conference on Soil Mechanics and Foundation Engineering*. 1.1. pp. 229–236.
- Leonardi, N., Ganju, N.K., Fagherazzi, S., 2016. A linear relationship between wave power and erosion determines salt-marsh resilience to violent storms and hurricanes. *Proc. Natl. Acad. Sci.* 113 (1), 64.
- Lin, M.-Y., Hagler, G., Baldauf, R., Isakov, V., Lin, H.-Y., Khlystov, A., 2016. The effects of vegetation barriers on near-road ultrafine particle number and carbon monoxide concentrations. *Sci. Total Environ.* 553, 372–379.
- Lunne, T., Powell, J.J.M., Robertson, P.K., 1997. *Cone Penetration Testing in Geotechnical Practice*. CRC Press.
- Mack, J.J., 2001. *Ohio Rapid Assessment Method for Wetlands V. 5.0, User's Manual and Scoring Forms*. Ohio EPA Technical Report WET/2001-1. Ohio Environmental Protection Agency, Division of Surface Water, Wetland Ecology Group, Columbus, Ohio.
- Marchetti, S., 1980. In-situ tests by flat dilatometer. *J. Geotech. Eng.* 106 (3), 299–321.
- Mariotti, G., Fagherazzi, S., 2010. A numerical model for the coupled long-term evolution of salt marshes and tidal flats. *J. Geophys. Res.: Earth Surface* 115 (F1).
- Mayne, P.W., 2007. NCHRP Synthesis 368: Cone Penetration Testing. Transportation Research Board, Washington, DC, pp. 118.
- McClenahan, G., Eugene Turner, R., Tweel, A.W., 2013. Effects of oil on the rate and trajectory of Louisiana marsh shoreline erosion. *Environ. Res. Lett.* 8 (4), 044030.
- McGinnis, Thomas E., 1997. *Shoreline Movement and Soil Strength in a Louisiana Coastal Marsh*. University of Louisiana at Lafayette.
- McKee, K.L., McGinnis II, T.E., 2003. Hurricane Mitch: effects on mangrove soil characteristics and root contributions to soil stabilization (2003-178). Retrieved from: <http://pubs.er.usgs.gov/publication/of03178>.
- Meijer, G.J., Bengough, A.G., Knappett, J.A., Loades, K.W., Nicoll, B.C., 2015. *New in Situ Techniques for Measuring the Properties of Root-Reinforced Soil – Laboratory Evaluation*, vol. 66. pp. 27–40 1.
- Meijer, G.J., Bengough, G., Knappett, J., Loades, K., Nicoll, B., 2017a. In Situ Root Identification through Blade Penetrometer Testing – Part 2: Field Testing, vol. 68. pp. 320–331 4.
- Meijer, G.J., Bengough, G., Knappett, J., Loades, K., Nicoll, B., Mukov, I., Zhang, M., 2017b. In Situ Root Identification through Blade Penetrometer Testing – Part 1: Interpretative Models and Laboratory Testing, vol. 68. pp. 303–319 4.
- Menard, L., 1975. The Menard Pressuremeter: Interpretation and Application of the Pressuremeter Test Results to Foundations Design. *Sols-Soils*, No 26.
- Mendez, F.J., Losada, I.J., 2004. An empirical model to estimate the propagation of random breaking and nonbreaking waves over vegetation fields. *Coast Eng.* 51 (2), 103–118.
- Merrifield, C.M., 1980. *Factors Affecting the Interpretation of the In-Situ Shear Vane Test*. University of Surrey, Guildford, Surrey Doctor of Philosophy.
- Mesri, G., Ajlouni, M., 2007. Engineering properties of fibrous peats. *J. Geotech. Geoenviron. Eng.* 133 (7), 850–866.
- Mesri, G., Huvaj, N., 2007. Shear strength mobilized in undrained failure of soft clay and silt deposits. *Geotechnical Special Publication* (173). [https://doi.org/10.1061/40917\(236\)1](https://doi.org/10.1061/40917(236)1).
- Mesri, G., Shahien, M., 2003. Residual shear strength mobilized in first-time slope failures. *J. Geotech. Geoenviron. Eng.* 129 (1), 12–31.
- Mesri, G., Stark, T.D., Ajlouni, M.A., Chen, C.S., 1997. Secondary compression of peat with or without surcharging. *J. Geotech. Eng. Div., ASCE* 123 (5), 411–421.
- Micheli, E.R., Kirchner, J.W., 2002. Effects of wet meadow riparian vegetation on streambank erosion. 2. Measurements of vegetated bank strength and consequences for failure mechanics. *Earth Surf. Process. Landforms* 27 (7), 687–697.
- Morris, J.T., Sundareswar, P.V., Nietch, C.T., Kjerfve, B., Cahoon, D.R., 2002. Responses of coastal wetlands to rising sea level. *Ecology* 83, 2869–2877.
- Morris, J.T., Shaffer, G.P., Nyman, J.A., 2013. Brinson review: perspectives on the influence of nutrients on the sustainability of coastal wetlands. *Wetlands* 33, 975–988.
- Nestlerode, J.A., Engle, V.D., Bourgeois, P., Heitmuller, P.T., Macauley, J.M., Allen, Y.C., 2009. An integrated approach to assess broad-scale condition of coastal wetlands—the Gulf of Mexico Coastal Wetlands pilot survey. *Environ. Monit. Assess.* 150 (1), 21–29.
- Noorany, I., 1984. Phase relations in marine soils. *J. Geotech. Eng.* 110 (4), 539–543.
- Nuttle, W.K., Hemand, H.F., 1988. Salt marsh hydrology: implications for biogeochemical fluxes to the atmosphere and estuaries. *Glob. Biogeochem. Cycles* 2 (2), 91–114.
- Nyman, J.A., 2014. Integrating successional ecology and the delta lobe cycle in wetland research and restoration. *Estuar. Coasts* 37, 1490–1505.
- Pant, Hem Raj, 2013. *Erosional resistance of cohesive sediments in coastal saltmarshes*. LSU Master's Theses. https://digitalcommons.lsu.edu/gradschool_theses/386.
- Pestrong, R., 1972. Tidal-flat sedimentation at cooley landing, Southwest San Francisco bay. *Sediment. Geol.* 8 (4), 251–288.
- Pierce, R.S., Day Jr., J.W., Conner, W.H., Ramchran, E., Boumans, B.M., 1985. *A Comprehensive Wetland Management Plan for the LaBranche Wetland*, St. Charles Parish, Louisiana. Coastal Ecology Institute, Louisiana State University, Baton Rouge, LA.
- Pollen, N., 2007. Temporal and spatial variability in root reinforcement of streambanks: accounting for soil shear strength and moisture. *Catena* 69, 197–205.
- Quirk, T.E., Graham, S.A., Mendelssohn, I.A., Shaffer, G., Snedden, G., Twilley, R.R., Pahl, J., Lane, R., Day, J.W., 2019. Response of coastal wetland plants and soils to freshwater, sediment, and nutrient inputs: will Mississippi River sediment diversions enhance Louisiana wetlands. *Estuar. Coast Shelf Sci.*
- Randolph, M.F., 2004. Characterization of soft sediments for offshore applications. In:

- Proc. of 2nd Int. Conf. on Geotechnical and Geophysical Site Characterization, ISC'2, Porto. 1. pp. 209–232 (Millpress).
- Redfield Alfred, C., 1972. Development of a new England salt marsh. *Ecol. Monogr.* 42 (2), 201–237.
- Roctest, 2011. Instruction Manual: Field Inspection Vane Tester Model H-60. Instruction Manual: Field Inspection Vane Tester Model H-60. Roctest Limited.
- Sasser, C.E., Evers-Hebert, E., Milan, B., Holm Jr., G.O., 2013. Relationships of Marsh Soil Strength to Vegetation Biomass. Final Report to the Louisiana Coastal Protection and Restoration Authority (CPRA) through State of Louisiana Interagency Agreement No. 2503-11-45.
- Sasser, C.E., Evers-Hebert, E., Holm, G.O., Milan, B., Sasser, J.B., Peterson, E.F., DeLaune, R.D., 2018. Relationships of marsh soil strength to belowground vegetation biomass in Louisiana coastal marshes. *Wetlands* 38 (2), 401–409.
- Schlue Benjamin, F., et al., 2010. Influence of shear rate on undrained vane shear strength of organic harbor mud. *J. Geotech. Geoenviron. Eng.* 136 (10), 1437–1447.
- Schmertmann, J.H., 1986. Dilatometer to compute foundation settlement. In: *Use of In-Situ Tests in Geotechnical Engineering*, GSP, vol. 6. ASCE, Reston/VA, pp. 303–321.
- Shaffer, G.P., Day, J.W., Hunter, R.G., Lane, R.R., Lundberg, C.J., Wood, W.B., Hillman, E.R., Day, J.N., Strickland, E., Kandalepas, D., 2015. System response, nutria herbivory, and vegetation recovery of a wetland receiving secondarily-treated effluent in coastal Louisiana. *Ecol. Eng.* 79, 120–131.
- Snedden, G.A., Cretini, K., Patton, B., 2015. Inundation and salinity impacts to above-and belowground productivity in *Spartina patens* and *Spartina alterniflora* in the Mississippi River deltaic plain: implications for using river diversions as restoration tools. *Ecol. Eng.* 81, 133–139.
- Stark, T.D., Delashaw, J.E., 1990. Correlations of unconsolidated undrained triaxial tests and cone penetration tests. *Transp. Res. Rec.* 1278, 96–102 National Research Council, Transportation Research Board, Washington, D.C.
- Swarzenski, C.M., Doyle, T.W., Fry, B., Hargis, T.G., 2008. Biogeochemical response of organic-rich freshwater marshes in the Louisiana delta plain to chronic river water influx. *Biogeochemistry* 90, 49–63.
- Syvitski, J.P.M., Kettner, A.J., Overeem, I., Hutton, E.W.H., Hannon, M.T., Brakenridge, G.R., Day, J., Vörösmarty, C., Saito, Y., Giosan, L., Nicholls, R.J., 2009. Sinking deltas due to human activities. *Nat. Geosci.* 2, 681.
- Terzaghi, K., Fröhlich, O.K., 1936. *Theorie der Setzung von Tonschichten*. Franz Deuticke, Leipzig.Voyiadjis.
- Terzaghi, K., Peck, R.B., Mesri, G.M., 1996. *Soil Mechanics in Engineering Practice*. J. Wiley & Sons; Chapman & Hall, New York; London.
- Thorne, C.R., 1990. Effects of vegetation on riverbank erosion and stability. In: Thorne, J.B. (Ed.), *Vegetation and Erosion*. Wiley, Chichester, pp. 125–143.
- Turner, R.E., 2011. Beneath the salt marsh canopy: loss of soil strength with increasing nutrient loads. *Estuar. Coasts* 34, 1–10.
- Turner, R.E., Howes, B.L., Teal, J.M., Milan, C.S., Swenson, E.M., Goehringer-Toner, D.D., 2009. Salt marshes and eutrophication: an unsustainable outcome. *Limnol. Oceanogr.* 54, 1634–1642.
- Turner, R.E., Bodker, J.E., Schulz, C., 2018. The belowground intersection of nutrients and buoyancy in a freshwater marsh. *Wet. Ecol. Manag.* 26 (2), 151–159.
- Twohig, T.M., Stolt, M.H., 2011. Soils-Based Rapid Assessment for Quantifying Changes in Salt Marsh Condition as a Result of Hydrologic Alteration. *Wetlands* 31 (5), 955.
- USACE, 1958. *Geology of the Mississippi River Deltaic Plain, Southeastern Louisiana*. U.S. Army Engineer Waterways Experiment Station.
- Van Eerd, M.M., 1985. Salt marsh cliff stability in the oosterschelde. *Earth Surf. Process. Landforms* 10 (2), 95–106.
- Van Zomeren, C.M., White, J.R., DeLaune, R.D., 2011. Fate of nitrate in vegetated brackish coastal marsh. *Soil Sci. Soc. Am. J.* 76, 1919–1927.
- Vuik, V., Jonkman, S.N., Borsje, B.W., Suzuki, T., 2016. Nature-based flood protection: the efficiency of vegetated foreshores for reducing wave loads on coastal dikes. *Coast Eng.* 116, 42–56.
- Wardrop, D.H., Kentula, M., Stevens, D.L., Jensen, S.F., Brooks, R., 2007. Assessment of wetland condition: an example from the Upper Juniata watershed in Pennsylvania, USA. *Wetlands* 27, 416–430.
- Wdowinski, Shimon, Hong, Sang-Hoon, 2015. *Wetland InSAR: A Review of the Technique and Applications*. <https://doi.org/10.1201/b18210-10>.
- Wigand, C., Roman Charles, T., Davey, E., Stolt, M., Johnson, R., Hanson, A., Watson Elizabeth, B., Moran, S.B., Cahoon Donald, R., Lynch James, C., Rafferty, P., 2014. Below the disappearing marshes of an urban estuary: historic nitrogen trends and soil structure. *Ecol. Appl.* 24 (4), 633–649.
- Wigand, C., Watson, E.B., Martin, R., Johnson, D.S., Warren, R.S., Hanson, A., Davey, E., Johnson, R., Deegan, L., 2018. Discontinuities in soil strength contribute to destabilization of nutrient-enriched creeks. *Ecosphere* 9 (8), e02329.
- Wilson, C.A., Hughes, Z.J., FitzGerald, D.M., 2012. The effects of crab bioturbation on Mid-Atlantic saltmarsh tidal creek extension: geotechnical and geochemical changes. *Estuar. Coast Shelf Sci.* 106, 33–44.
- Yafraite, N., DeJong, J., DeGroot, D., Randolph, M., 2009. Evaluation of remolded shear strength and sensitivity of soft clay Using Full-Flow Penetrometers. 135 (9), 1179–1189.
- Yu, H.S., Mitchell, J.K., 1998. Analysis of cone resistance: review of methods. *J. Geotech. Geoenviron. Eng.* ASCE. 124 (2), 140–149.
- Zeeb, P., 1997. Piezocone Mapping, Groundwater Monitoring, and Flow Modeling in a Riverine Peatland: Implications for the Transport of Arsenic.
- Zhao, H., Chen, Q., 2013. Modeling attenuation of storm surge over deformable. *Veg.: Methodol. Verif.* 140 (12), 04014090.
- Peck, R.B., 1967. *Stability of Natural Slopes*. Journal of Soil Mechanics and Foundations Division, American Society of Civil Engineers, New York 93 (SM4), 403–417.